Comprehensive estimation of lake volume changes on the Tibetan Plateau during 1976–2019 and basin-wide glacier contribution

Guoqing Zhang [a,b,*], Tobias Bolch [c], Wenfeng Chen [a,e], Jean-François Crétaux [d]

[a] *Key Laboratory of Tibetan Environmental Changes and Land Surface Processes, Institute of Tibetan Plateau Research, Chinese Academy of Sciences (CAS), Beijing, China*

[b] *CAS Center for Excellence in Tibetan Plateau Earth Sciences, Beijing, China*

[c] *School of Geography and Sustainable Development, University of St Andrews, St Andrews, Scotland, UK*

[d] *LEGOS, Université de Toulouse CNES, CNRS, IRD, UPS, F-31400 Toulouse, France*

[e] *University of Chinese Academy of Sciences, Beijing, China*

* Correspondence author at: Key Laboratory of Tibetan Environmental Changes and Land Surface Processes, Institute of Tibetan Plateau Research, Chinese Academy of Sciences (CAS), Beijing, China

E-mail address: guoqing.zhang@itpcas.ac.cn (G. Zhang)

Abstract:

Volume changes and water balances of the lakes on the Tibetan Plateau (TP) are spatially heterogeneous and the lake-basin scale drivers remain unclear. In this study, we comprehensively estimated water volume changes for 1132 lakes larger than 1 km^2 and determined the glacier contribution to lake volume change at basin-wide scale using satellite stereo and multispectral images. Overall, the water mass stored in the lakes increased by 169.7±15.1 Gt (3.9±0.4 Gt yr^{-1}) between 1976 and 2019, mainly in the Inner-TP (157.6±11.6 or 3.7±0.3 Gt yr^{-1}). A substantial increase in mass occurred between 1995 and 2019 (214.9±12.7 Gt or 9.0±0.5 Gt yr^{-1}), following a period of decrease (-45.2±8.2 Gt or -2.4±0.4 Gt yr^{-1}) prior to 1995. A slowdown in the rate of water mass increase occurred between 2010 and 2015 (23.1±6.5 Gt or 4.6±1.3 Gt yr^{-1}), followed again by a high value between 2015 and 2019 (65.7±6.7 Gt or 16.4±1.7 Gt yr^{-1}). The increased lake-water mass occurred predominately in glacier-fed lakes (127.1±14.3 Gt) in contrast to non-glacier-fed lakes (42.6±4.9 Gt), and in endorheic lakes (161.9±14.0 Gt) against exorheic lakes (7.8±5.8 Gt) over 1976−2019. Endorheic and glacier-fed lakes showed strongly contrasting patterns with a remarkable storage increase in the northern TP and slight decrease in the southern TP. The ratio of excess glacier meltwater runoff to lake volume increase between 2000 and ~2019 was less than 30% for the entire Inner-TP based on several independent data sets. Among individual lake-basins, 14 showed a glacier contribution to lake volume increase of 0.3% to 29.1%. The other eight basins exhibited a greater glacier contribution of 116% to 436%, which could be explained by decreased net precipitation. The lake volume change and basin scale glacier contribution reveal that the enhanced precipitation predominantly drives lake volume increase but it is spatially heterogeneous.

Key words: lake volume change, glacier mass balance, lake water balance, Tibetan Plateau

1. Introduction

Lakes are an important water resource and component of the global water cycle in the world, besides rivers, wetlands and glaciers (Marzeion et al., 2014; Niu et al., 2011; Pekel et al., 2016; Yamazaki et al., 2015). The dense distribution of large lakes in the Tibetan Plateau (TP), the highest and largest plateau on Earth, has drawn the attention of scientists in hydrology, remote sensing and climatology. They are attracted by the natural state (i.e., without disturbance by human-activities) of these lakes, their integration with the cryosphere, and their sensitivity to global climate change (Crétaux et al., 2016; Pekel et al., 2016; Phan et al., 2012; Rüthrich et al., 2015). The lakes on the TP account for an important fraction of water storage and can affect the atmosphere's circulation and climate change at regional and even hemispherical scale (Dai et al., 2018; Rüthrich et al., 2015; Zhu et al., 2018). At the same time, these lakes act as an indicator and/or regulator of climate change (Samuelsson et al., 2010; Williamson et al., 2009). The TP has warmed, possibly three times faster than the global average (Duan et al., 2015). The climate over the TP has also become wetter (Yang et al., 2011), which is reflected in lake growth (Treichler et al., 2019; Zhang et al., 2019), vegetation greening (Zhang et al., 2017d; Zhong et al., 2019; Zhu et al., 2016), and increased groundwater storage (Xiang et al., 2016; Yi et al., 2016; Zhang et al., 2017b).

The large amount of satellite remote sensing data now available allows monitoring of changes in the surface areas of plateau lakes (Zhang et al., 2019), their levels (Phan et al., 2012; Zhang et al., 2011) and volumes (Crétaux et al., 2016; Song et al., 2013; Yang et al., 2017; Yao et al., 2018), and their responses to climate change by measuring surface water temperatures and lake ice phenology (Zhang et al., 2020). The most extensive studies have been on the temporal and spatial variations of lake areas. Lake level changes are restricted to a small number of lakes (<150 out of the ~1200 lakes in the TP; inset of Fig. 1) covered with altimetry data (Crétaux et al., 2011; Jiang et al., 2017; Kleinherenbrink et al., 2015; Phan et al., 2012). The lake volume change is usually estimated by combining surface area and water level change, which is only reported for large lakes (>10 km^2) or limited time spans (Qiao et al., 2019b; Song et al., 2013; Yang et al., 2017; Yao et al., 2018; Zhang et al., 2017b). The overall lake volume change is estimated by upscaling, using the area ratio of all lakes (>1 km^2) to lakes with available altimetry data (Song et al., 2013; Zhang et al., 2017b). Despite our comprehensive knowledge of lake-water storage changes and spatial patterns during the second half of the 20th century, we still have limited understanding of lake evolution, their water balances and roles in the hydrological cycle.

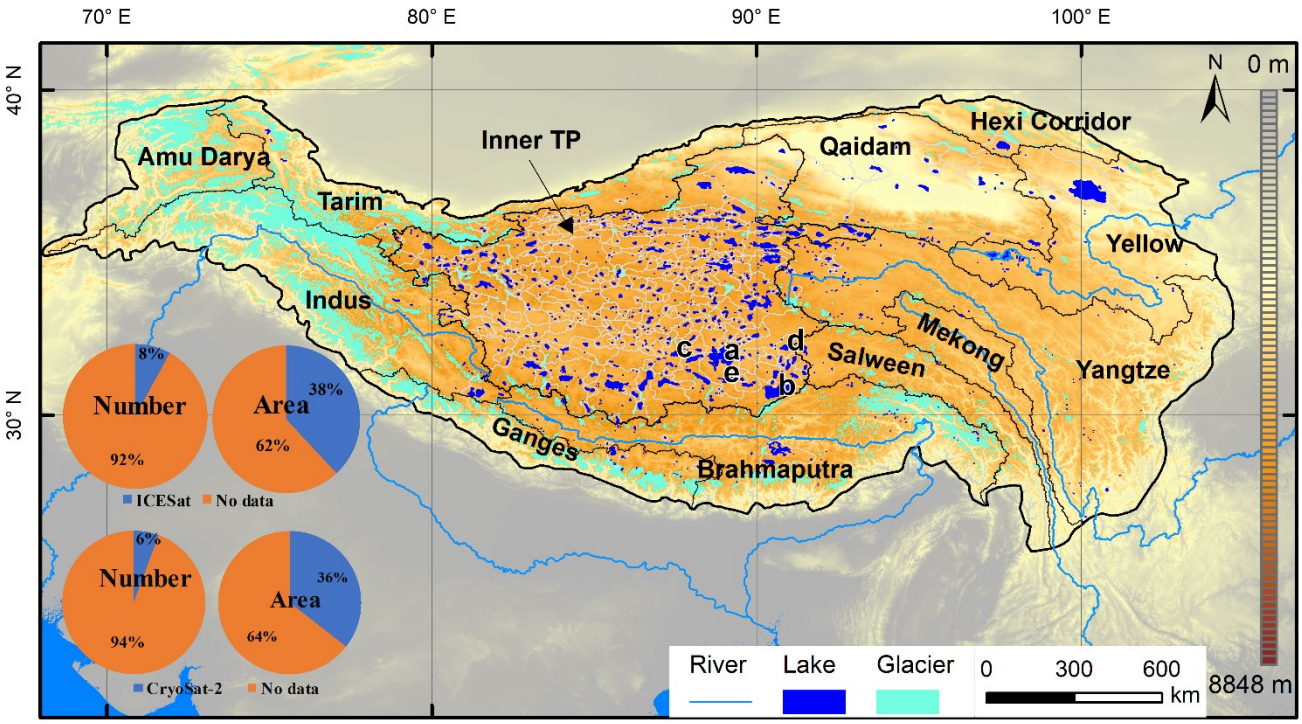

Fig. 1. Spatial distribution of lakes, glaciers, and rivers and their basins on the Tibetan Plateau (TP) and surroundings. The boundary of TP is derived from SRTM DEM at the altitude of 2500 m a.s.l. The ratios of number and area of lakes with surface elevation measurements from ICESat and CryoSat-2 altimetry data to total lakes (>1 km^2) are shown in blue as insets in lower left. The letters "a, b, c, d, e" indicate the locations of lakes shown in Fig. 7. The glacier outlines are from the Randolph Glacier Inventory (RGI, v5.0) (Pfeffer et al., 2014). No changes were made between RGI v5.0 and v6.0 in the investigating region (RGI-Consortium, 2017).

The lake area, level and volume changes on the TP have increased rapidly in recent decades (Zhang et al., 2020). These changes raise some important questions: what is the dominant driver, cryosphere (glacier, snow, permafrost) or atmospheric changes (precipitation, evaporation); and what is the respective contribution from each of these factors? A quantitative assessment of lake water balance by hydrological model has been conducted for only a few lakes, such as Nam Co, Selin Co, Mapam Yumco, Tangra Yumco, Paiku Co (Biskop et al., 2016; Li et al., 2017a; Tong et al., 2020; Zhou et al., 2015; Zhou et al., 2019). Satellite geodetic method has also been used for estimation of glacier mass loss to water gains of limited lakes such as Nam Co, LexieWudan Lake, and KekeXili Lake (Li et al., 2017b; Zhou et al., 2019). Hence, our knowledge of lake water balances at lake-basin scale across the entire TP remains poorly quantified. This knowledge gap is because of the limited meteorological and hydrological observations, the uneven

weather station distribution as most of these stations are concentrated in the eastern TP, and the uncertainties in satellite-based precipitation products (Behrangi et al., 2017; Tong et al., 2014; Wortmann et al., 2018). Although a previous study has roughly estimated lake water balance for the Inner-TP as a whole (Zhang et al., 2017b), the overall basin-scale lake-water balances and their spatial differences are still unknown. A consistent spatially-resolved estimate of glacier mass balance (Brun et al., 2017) provides the possibility to evaluate lake water balance from glacier contribution.

The aim of this study is to comprehensively estimate water volume change for each lake larger than 1 km^2 from 1976 to 2019 using digital elevation data in addition to measuring their area and level changes using optical satellite imagery and radar altimetry data. These changes include the analysis of lake volume changes at lake-basin scale, long-term evolution and spatial patterns (differences between glacier-fed and non-glacier-fed, endorheic and exorheic lakes). Moreover, the contributions of glacier mass change to lake volume change at lake-basin scale and for the entire Inner-TP were quantified. The correlation between precipitation and lake volume variation was also examined and evaluated.

2. Study area

The TP covers an area of approximately 3×10^6 km^2, with a mean elevation in excess of 4000 m a.s.l. There are ~1200 lakes with an area greater than 1 km^2, with a total area of ~47,000 km^2 in 2010 (Fig. 1). There are 95 China Meteorological Administration (CMA) meteorological stations with observations during the last two decades, of which 49 have been operating since the 1950s (Li et al., 2009). However, these stations are mainly distributed in the eastern TP and at relatively low altitudes (<4800 m a.s.l.), which does not correspond with the spatial distribution of the lakes. Climate in the TP in the past decades has become warmer and wetter (Kuang et al., 2016; Yang et al., 2011). The air temperature increased at a rate of 0.04±0.005 ^oC yr^{-1} in 1980–2018 (Zhang et al., 2019). The TP is divided into 12 large river/lake basins: Inner-TP, Qaidam, Hexi Corridor, Yellow, Yangtze, Mekong, Salween, Brahmaputra, Ganges, Indus, Amu Darya, Tarim (Fig. 1).

3 Data and methodology

3.1. Landsat imagery and SRTM DEM for lake volume change

Lake areas between 1976 and 2019 are derived from Landsat MSS/TM/ETM+/OLI data downloaded from https://glovis.usgs.gov/ (Table S1). Landsat data for stable lake area and low cloud coverage in September–November (Yu et al., 2016) are selected to decrease within-year variability. Lake boundaries from Landsat MSS (~60 m pixel size resampled) were manually delineated as the image quality were too low for automated processing. Firstly, the original digital number (DN) value of Landsat imagery is converted to top-of-the-atmosphere (TOA) reflectance (Li et al., 2012). For times and regions with no suitable Landsat TM imagery we used Landsat 7 ETM+ SLC-off data instead. The data gaps were filled using local linear histogram matching developed by Scaramuzza et al. (2004). Secondly, the normalized difference water index (NDWI) (McFeeters, 1996) is used to generate a binary image separating water bodies from non-water components. The optimal thresholds determined from the Otsu method (Otsu, 1979) are used to distinguish water from non-water features. Each lake water unit is visually edited in combination with the original Landsat imagery if it is not extracted exactly by semi-automatic water classification. Finally, each lake's area is calculated and its features are labeled (Latitude, Longitude, Number, Name, Area, Elevation) for comparative analysis.

The Shuttle Radar Topography Mission (SRTM) produced digital elevation models (DEMs) of the Earth between 60 ^{o}N and 57 ^{o}S by interferometric synthetic aperture radar (InSAR) between 11 and 22 February 2000 (Farr et al., 2007; Rabus et al., 2003). The SRTM provides a nearly global high-quality DEMs at the spatial resolutions of 1 and 3 arc sec (~30 and ~90 m), with vertical absolute error of <16 m (relative vertical accuracy of <6 m) and absolute geolocation error of <20 m (Farr et al., 2007). Many studies have evaluated the accuracy of SRTM DEM, and found it is better than mission specification, as verified globally (Bhang et al., 2007; Farr et al., 2007; Rodriguez et al., 2006). In this study, the 1 arc sec SRTM DEM (v1) covering the entire TP (via https://search.earthdata.nasa.gov/) was used.

The homogeneous high-resolution SRTM DEM provides the possibility of reconstructing lake levels using satellite measured inundation areas (Qiao et al., 2019a; Treichler et al., 2019; Yang et al., 2017). We estimated lake levels based on the SRTM DEM using an Elevation-Area correlation (Fig. 2). The lake boundaries derived from Landsat data in 2015 were selected to create a buffer zone outside (5 km, assumed as the maximum expanding distance). The pixels with the lowest elevation within the buffered lake basin zone are first selected. The altitude is elevated by 1 m, the corresponding inundation area is then recorded. The stepwise iteration will stop when the elevation has been increased by 20 m, which is greatly higher than the maximum lake level rise (<10 m) in the study period (Zhang et al., 2011). The pixels with abnormal elevation values are then removed using a Nine-Neighborhood-Maximum-Filter. In

addition, the lake area from Landsat in 2000 is employed as a reference to check if the lake area derived from the SRTM DEM is reliable. The correlation (r^2) and root-mean-square error (RMSE) between lake area and level is used to test if the constructed relationship based on SRTM DEM is reasonable (Fig. S1). The lake area from the multi-temporal Landsat data was inputted into an Elevation-Area correlation to deduce the corresponding lake level.

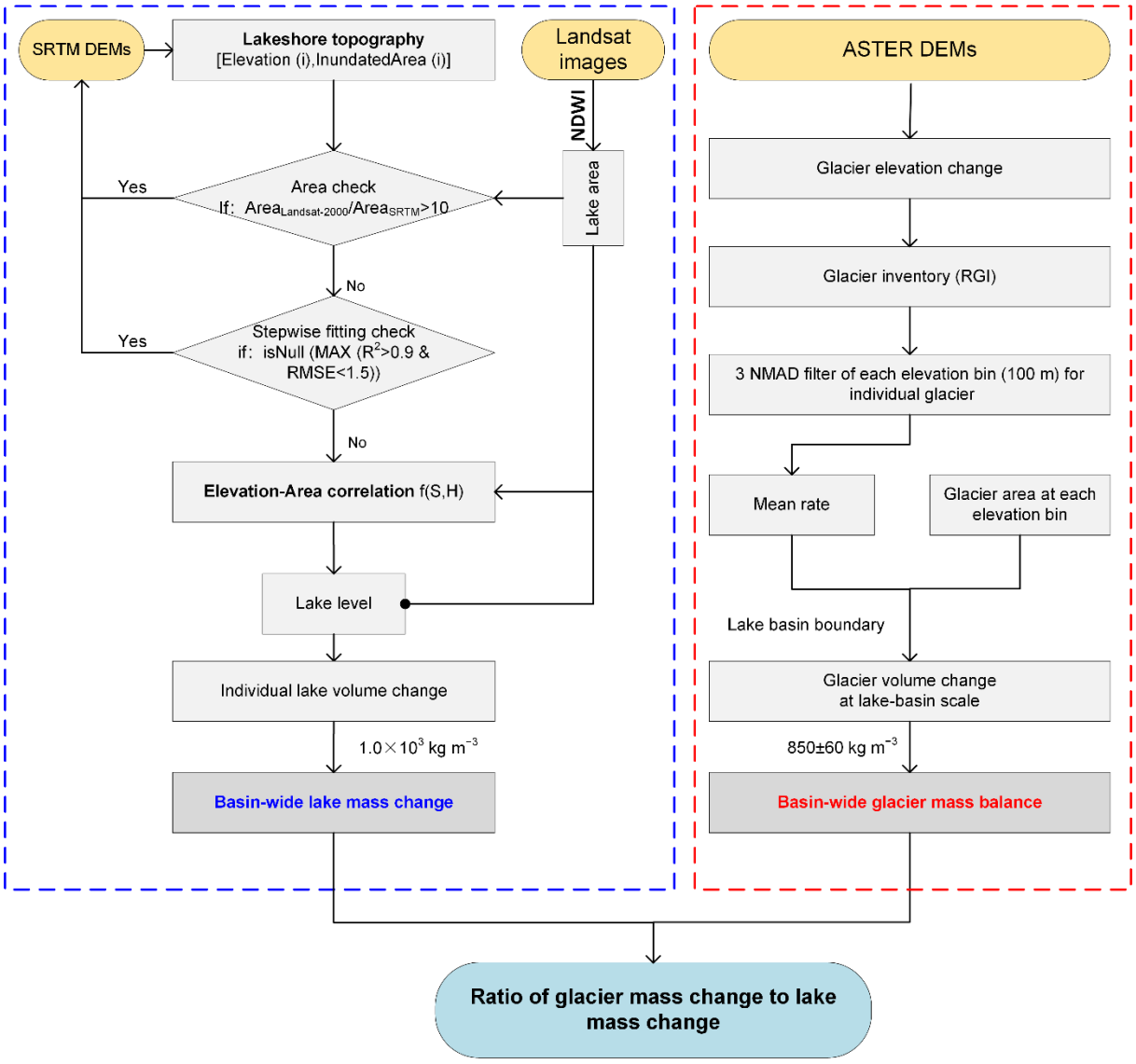

Fig. 2. Flow chart showing the estimation for both lake mass (volume) change and glacier mass balance.

Lake level derived from the SRTM DEM has a vertical resolution of 1 m. However, we reconstruct the correlation between lake area and level, and to retrieve high accuracy lake levels from Landsat-observed lake areas. In addition, this algorithm is applicable regardless if lakes are expanding or shrinking. Excluding some lakes with abnormal lake

level changes (with pairs of Elevation-Area correlation less than 5) as topographic factor, 1132 lakes of greater than 1 km^2 have available data. Combining lake level and area, the change of water volume for an individual lake is then calculated using Equation (1).

$$\Delta V = \frac{1}{3}(H_2 - H_1) \times (A_1 + A_2 + \sqrt{A_1 \times A_2}) \quad (1)$$

where ΔV is the change in lake volume. The H_1, A_1 and H_2, A_2 are lake level and area on the beginning and end dates between two periods. The effects of sediment transported by the glaciers into the lake in estimating lake volume change are not involved considering the cold environment as the sediment load is probably very small in the TP interior with majority of lakes (e.g. Tian et al., 2020). Changes of lake volume along with lake level and area for 1132 lakes are estimated separately. Lake volume change is further converted to mass change combining with water density of 1.0×10^3 kg m^{-3} at 4 °C.

Lake basin boundaries were extracted from HydroSHEDS (Hydrological data and maps based on SHuttle Elevation Derivatives at multiple Scales, http://hydrosheds.org/). If a lake basin outline was not available from HydroSHEDS, it was delineated from the SRTM DEM using hydrology tool (Watershed) in the ArcGIS toolbox. All lake basin boundaries were examined and edited in combination with the SRTM DEM and Google Earth imagery. Lakes were classified into exorheic (lakes with water flowing in as well as flowing out, or lakes with water flowing out only) or endorheic (lakes without water flowing out). Lakes were also categorized as glacier-fed or non-glacier-fed according to whether there is a glacier stream flowing into the lake from a glacier terminus. Google Earth and the China's river dataset are applied to assist with the glacier-fed/non-glacier-fed lake classification.

3.2. Validation of estimated lake volume change

For validation we compared lake areas from SRTM DEM and Landsat data of 2000. The SRTM DEM performed well at retrieving lake area (Fig. 3a). However, it only provides a static snapshot of the lake areas for the year 2000. In addition, lake level changes from in situ measurements for Qinghai Lake (the only lake with long-term water level measurements in the TP) between 1976 and 2019 were also used to compare lake level retrieved from the SRTM DEM (Fig. 3b). The correlation (r^2) and RMSE between them are 0.96 and 0.66 m, respectively. We further compared lake level changes of SRTM/Landsat with ICESat data (Release-33) (Zhang et al., 2011) and CryoSat-2 data (Jiang et al., 2017). The overall correlations between them are also high (Fig. 3c–d). The ICESat data show a similar

performance (r^2=0.87, RMSE=0.86 m, mean error= 0.72 m) with CryoSat-2 (r^2=0.71, RMSE=0.61 m, mean error= 0.53 m).

In addition, lake volume changes from SRTM DEM present high accuracy (overall mean error of ~5%) for five lakes (Nam Co, Tangra Yumco, Taro Co, Buro Co and Gyado Co) in the TP when compared with in-situ bathymetric survey (Yang et al., 2017). Yao et al. (2018) shows a high consistency (r^2=0.97, <5% bias in aggregated storage change) of volume changes for 18 lakes derived from SRTM DEM and Hydroweb hypsometry (http://hydroweb.theia-land.fr/hydroweb) (Crétaux et al., 2016). The validations of lake level changes derived using our algorithm with in situ measurements and altimetry data prove that Area-Elevation correlations can retrieve reliable water level changes for lakes on the TP.

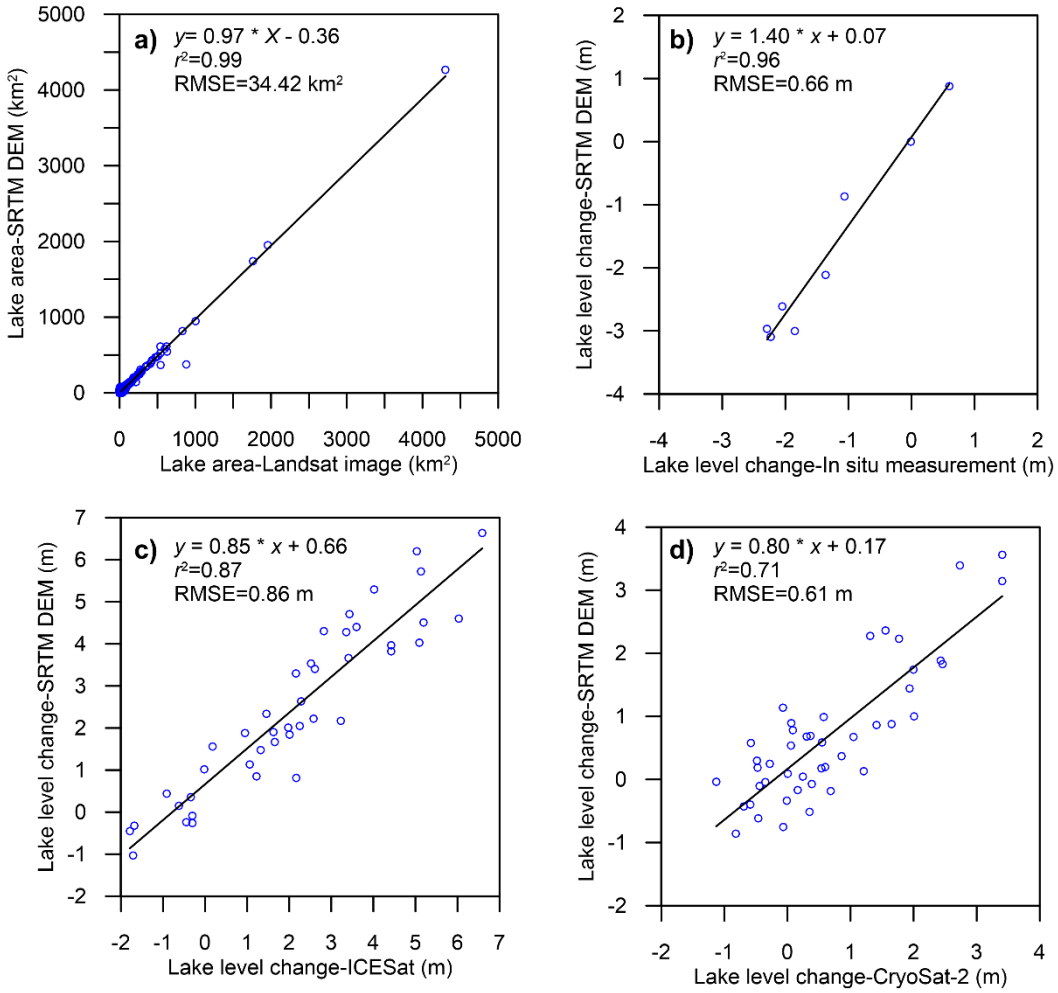

Fig. 3. Performances of SRTM DEM in lake area/level derivation in comparison to in situ measurements and satellite data. a) Comparison of lake area derived from SRTM DEM and Landsat image. b) Comparison of the water level changes of Qinghai Lake derived from SRTM DEM to in situ measurements from 1976, 1990, 1995, 2000, 2005,

2010, 2015, and 2019. c) Comparison of lake level changes derived from SRTM DEM and ICESat. d) Comparison of lake level changes derived from SRTM DEM and CryoSat-2.

3.3. ASTER DEMs for basin-scale glacier mass balance

Many studies have estimated glacier mass balance by the geodetic method (i.e. the elevation difference between multi-temporal DEMs) using the SRTM DEM as baseline data (Bolch et al., 2017; Gardelle et al., 2012; Li et al., 2017b) or using ICESat data (Gardner et al., 2013; Kääb et al., 2012; Neckel et al., 2014). SRTM-based estimates are however affected by radar penetration into snow and ice where ICESat-based estimates have a coarse coverage. ASTER optical stereo pairs can overcome these limitations. The pixel-based linear regression of ASTER DEMs (30 m) between 2000 and 2016 is used to estimate elevation changes of individual glaciers (Brun et al., 2017) (Fig. 2). Following the regional assessment of glacier mass balance (Brun et al., 2017; Shean et al., 2020), only the annual "excess discharge", i.e. the additional water due to glacier mass loss, is considered. The lake-basin scale glacier mass balance is further estimated (Fig. 2). Of the 132 lake basins with glacier coverage, 78 (59%) had satisfactory coverage with geodetic mass balance data derived from the ASTER imagery. The glacier coverages in the remaining 54 lake basins were too sparse and glaciers were too small to obtain significant results of glacier mass changes. The glacier contribution to lake volume change is finally evaluated for 22 basins with glacier mass loss and lake water gain as well as a high sampled glacier area (>70%).

3.4. Uncertainty of lake volume change and glacier mass balance

The uncertainties of lake volume change can be derived from lake area and water level estimations. Landsat imagery with a spatial resolution of 30 m for TM/ETM+/OLI sensors and ~60 m for MSS are used to derive lake area, which has been widely employed for lake mapping across the globe (Sheng et al., 2016; Verpoorter et al., 2014). The uncertainty of lake area delineations is estimated at ±0.5 pixels around the delineated lake boundary (Bolch et al., 2011; Fujita et al., 2009; Salerno et al., 2012; Wang et al., 2013). A comprehensive evaluation of the SRTM DEM derived lake levels for 1132 lakes shows a high correlation (r^2>0.9) and RMSE of less than 1.5 m between the inundated area and level. The uncertainty of lake volume change ($\sigma\Delta V_i$) is estimated according to Equation (2).

$$\sigma\Delta V_i = \sqrt{{\sigma_{H_1}}^2(\frac{\partial\Delta V}{\partial H_1})^2+{\sigma_{H_2}}^2(\frac{\partial\Delta V}{\partial H_2})^2+{\sigma_{A_1}}^2(\frac{\partial\Delta V}{\partial A_1})^2+{\sigma_{A_2}}^2(\frac{\partial\Delta V}{\partial A_2})^2} \quad (2)$$

where σ_{H_1}, σ_{H_2}, σ_{A_1}, σ_{A_1} are the uncertainties of elevation and area, respectively. In addition, some error sources are ignored due to limited available data. For example, low spatial resolution and limited accuracy of 30-m SRTM DEM data could result in potential uncertainties in deriving inundated area. The non-uniform lake bed slope could also induce potential error in estimating lake volume change when using Equation (1).

The uncertainties of glacier mass balance include random (the rate of elevation change, glacierized area, conversion of volume to mass balance) and systematic errors (absolute value of the triangulation residual) (Brun et al., 2017). These uncertainties are estimated for individual glacier and at lake-basin scale.

3.5. Precipitation change links with lake volume change

Yang et al. (2018) found that GPCC data perform better at retrieving the long-term trend of precipitation change in the Inner-TP compared to other products. Spatial and temporal patterns of precipitation changes from GPCC data between 1972 and 2015 are examined. The cumulative standardized precipitation is used to link with lake mass change, which shows a clearer turning point and trend of precipitation change, and could match better with relative lake mass change (a cumulative basin-wide water gain).

4. Results

4.1. Basin-wide lake and glacier distributions

Of the 1132 lakes examined, 379, 330 and 140 are endorheic, glacier-fed, and both endorheic and glacier-fed lakes, respectively (Table S2). These 1132 lakes are grouped into 429 basins delineated in this study (Fig. 4). The spatial patterns of basin scale lake and glacier distributions showed the basins with large lakes (>1000 km^2) in the TP are conspicuous. Most basins have total lake area of <500 km^2. Lakes are predominantly distributed in the Inner-TP, but some are also found in the southern TP and around Qinghai Lake in the Yellow River basin. Those basins with a relatively large ratio (>9%) of total lake area to lake basin area are mainly distributed in the south, northwest, and northeast of Inner-TP. Total glacier area in lake basins is generally small (<100 km^2) relative to lakes, excluding three basins (>400 km^2) in the northwest and northeast of Inner-TP. The ratio of total glacier area to lake basin area is also small (<3%) compared with lakes, excluding one lake basin (containing the Zangsar Kangri Glacier) in the center and several basins in the northwest of Inner-TP with ratios of >6%. The fractions of lakes and glacier distributions in each

245 basin can create local climate anomalies and affect the water balance at regional scale (Dai et al., 2018; Immerzeel et
246 al., 2020; Zhu et al., 2018).
247

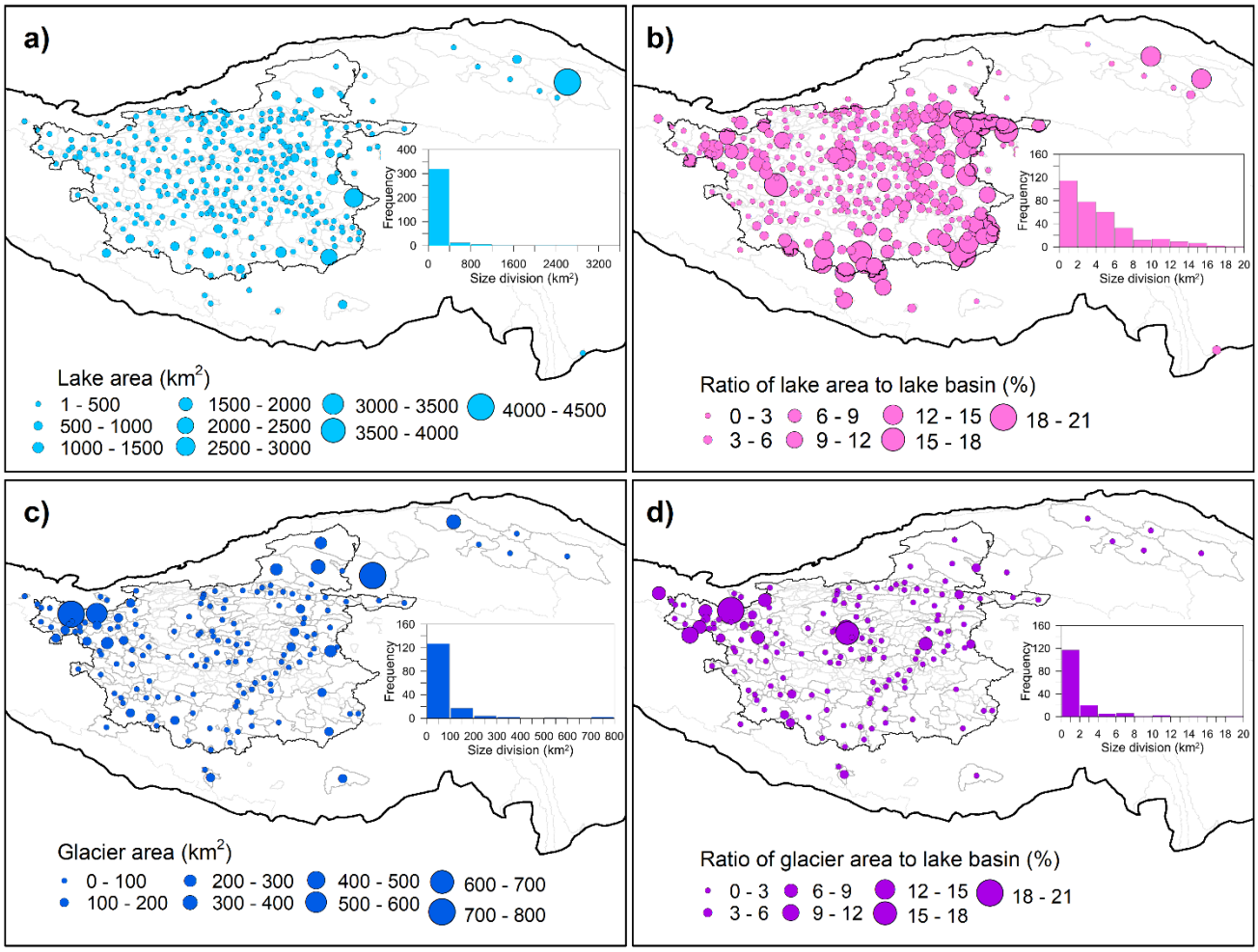

248

249 **Fig. 4.** Lakes in 2015 and glacier distributions from RGI v5.0 at lake-basin scale (429 basins are considered). a) Total
250 lake area at lake-basin scale. The inset shows the frequency of lake-basin scale lake area. b) Ratio of lake area to basin
251 area. The inset shows the frequency of ratio of lake area within each lake basin to basin area. c) Total glacier area at
252 lake-basin scale. The inset shows the frequency of lake-basin scale glacier area. d) Ratio of glacier area to lake basin.
253 The inset shows the frequency of ratio of glacier area within each lake basin to basin area.
254

255 ***4.2. Lake volume change***

256 The lakes greater than 1 km² (1132 lakes) are respectively examined for their volume changes between 1976 and
257 2019 (Table S2). They have a total net water mass increase of 169.7±15.1 Gt from 1976 to 2019 (Table 1, Table S3).

This total comprises an increase of 161.9±14.0 Gt for the endorheic lakes covering a total area of 34,075±38 km^2 (77% in area) and 7.8±5.8 Gt for the exorheic lakes (10,176±15 km^2, 23%). The glacier-fed lakes (32,332±34 km^2, 74%) revealed a water storage increase of 127.1±14.3 Gt larger than the 42.6±4.9 Gt for non-glacier-fed lakes (11919 ±17 km^2, 26%). Lakes with increased water mass change dominate those with decreases. The water storage has increased strongly for lakes that are both endorheic and glacier-fed (129.5±13.8 Gt). These numbers clearly highlight the differences of total water storage change for lakes with different sources of water supply.

Table 1 Lake water mass changes for endorheic, exorheic, glacier-fed and non-glacier-fed lakes between 1976 and 2019. Lake area in 2015 is used.

	All lakes	Endorheic	Exorheic	Glacier-fed	Non-glacier-fed	Endorheic & Glacier-fed
Lake area (km^2)	44251±41	34075±38	10176±15	32332±34	11919±17	27117±32
Increased mass (Gt)	263.1±12.3	231.3±11.4	31.8±4.6	197.6±11.5	65.5±4.2	184.3±11.2
Decreased mass (Gt)	-93.4±8.9	-69.4±8.1	-24.0±3.6	-70.5±8.5	-22.9±2.5	-54.8±8.0
Total mass change (Gt)	169.7±15.1	161.9±14.0	7.8±5.8	127.1±14.3	42.6±4.9	129.5±13.8

The lake volume changes at 12 large river basins of the TP (Fig. 5) showed that the Inner-TP has the largest magnitude of water mass change of 157.6±11.6 Gt between 1976 and 2019. In this basin, lakes lost -29.3±6.0 Gt in 1976 to 1995 period, before a mass increase of 186.8±9.9 Gt from 1995 to 2019. Lakes in the Yellow River basin show a similar shift in the water storage, i.e. -10.3±5.0 Gt before 1995 and 19.1±7.2 Gt in 1995–2019. Lakes in the Brahmaputra present the largest negative water storage change of -2.8±1.9 Gt in 1976–1995, with an overall negative water balance during the different evolution periods excluding 1995–2000 and 2015–2019. The magnitudes of lake water storage variations in other basins are small (<2 Gt), which could be due to the small number and area of lakes as well as water level changes. Lakes in the basins along the Himalayas are usually small glacier terminal lakes (<1.0 km^2), and not included in this study.

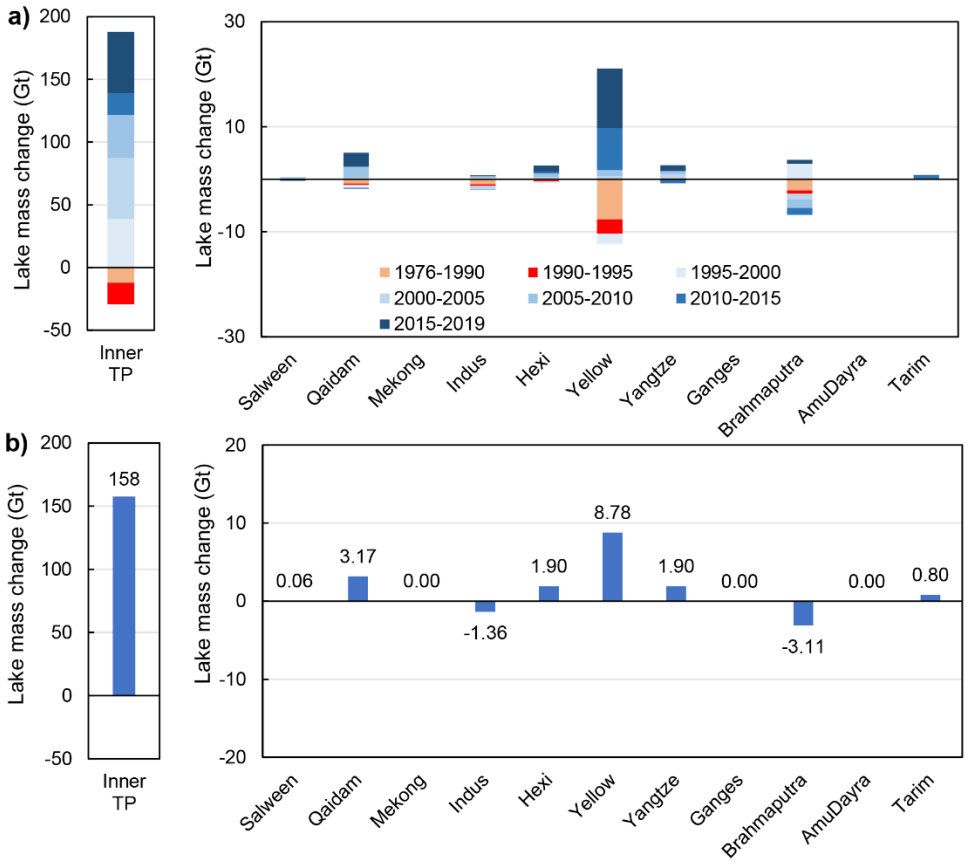

Fig. 5. Lake mass changes in 12 large river basins. Note that only the fraction of these basins located over the TP is examined here. a) Lake water mass changes for the seven periods in each basin. b) Total lake water mass changes between 1976 and 2019 for each basin. Note the strongly different vertical scale for the Inner-TP.

The time series of lake mass changes showed that the 1995 turning points are apparent for all types of lake (endorheic, exorheic, glacier-fed and non-glacier-fed lakes) (Fig. 6). Our 5-year sampling interval year, in order to cover small lakes (1–10 km^2) at the consistent period (with the minimum within-year variability), is limited to reveal whether a more precise inflection point of lake change occurred in 1997/1998 (Zhang et al., 2020). The endorheic and glacier-fed lakes indicate more negative changes of water loss than exorheic and non-glacier-fed lakes before 1995. However, water gained by endorheic and glacier-fed lakes far exceeded that gained by exorheic and non-glacier-fed lakes after 1995, respectively. The water mass changes are stable before 1995 for exorheic and non-glacier-fed lakes. A slowdown in lake water gain has appeared in several years (2010–2015), but a quick recovery occurred after 2015. The cumulative lake mass change shows a slight increase for non-glacier-fed lakes. However, it displayed a slight decrease in 1976–1995; which was followed by a continuous rapid increase of glacier-fed lakes. After 2005, glacier-

fed lakes exhibited a particularly larger water gain than non-glacier-fed lakes. For endorheic lakes against exorheic lakes, the exorheic ones indicated a stable trend of mass change from 1976 to 2019, but the endorheic lakes showed a slight decrease before 1995, then exceeded exorheic ones in 2000 and a continuous fast increase. The time series of cumulative lake mass change clearly illustrate the differences of lake evolution between glacier-fed and non-glacier-fed, and endorheic and exorheic lakes.

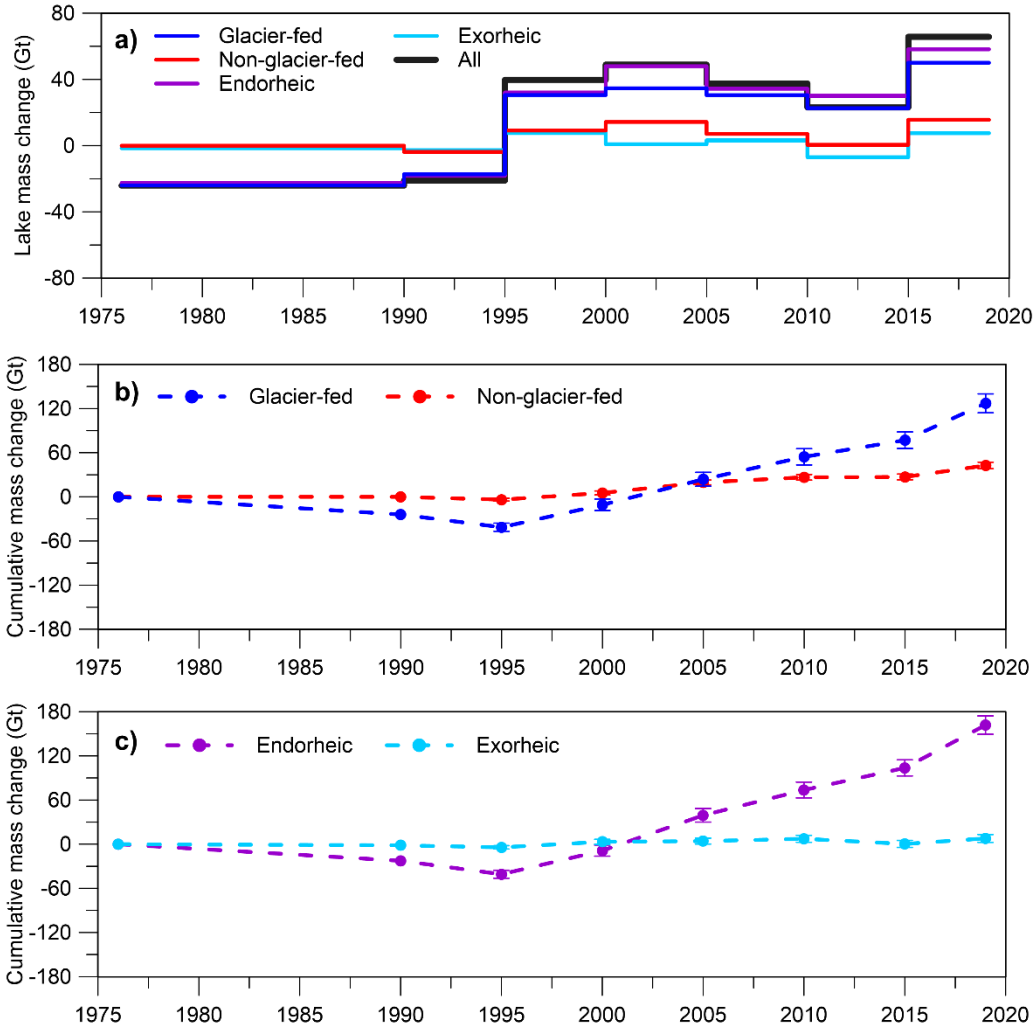

Fig. 6. Time series of lake mass changes relative to 1976. a) Water mass change for endorheic, exorheic, glacier-fed and non-glacier-fed lakes. b) Cumulative water mass change for glacier-fed and non-glacier-fed lakes. c) Cumulative water mass change for endorheic and exorheic lakes.

Five lakes in the Inner-TP, with different water recharge, have been selected to show the time series of lake area, level and volume changes (Fig. 7). Selin Co, an endorheic and glacier-fed lake, is the largest and fastest expanding lake in Tibet, experienced a water mass increase of ~23 Gt between 1976 and 2019. Nam Co, the second largest lake in Tibet, underwent increases in area, level and volume increase from 1995 to 2005, followed by a stable state in recent years. Dagze Co, an endorheic and glacier-fed lake, also showed continuous fast area, level and volume increases, especially since 2005. Zige Tangco, an endorheic lake, but with no glacier meltwater supply, also exhibited coherent area, level and volume rising. However, for Mugqu Co, an exorheic and non-glacier-fed lake, the area, level and volume showed a variable but decreasing trend. These examples demonstrate the coherent trends of lake area, level and volume changes across the TP. However, the patterns of lake evolution among different types of lakes during the past four decades are heterogeneous, especially for exorheic lakes with a decreasing trend.

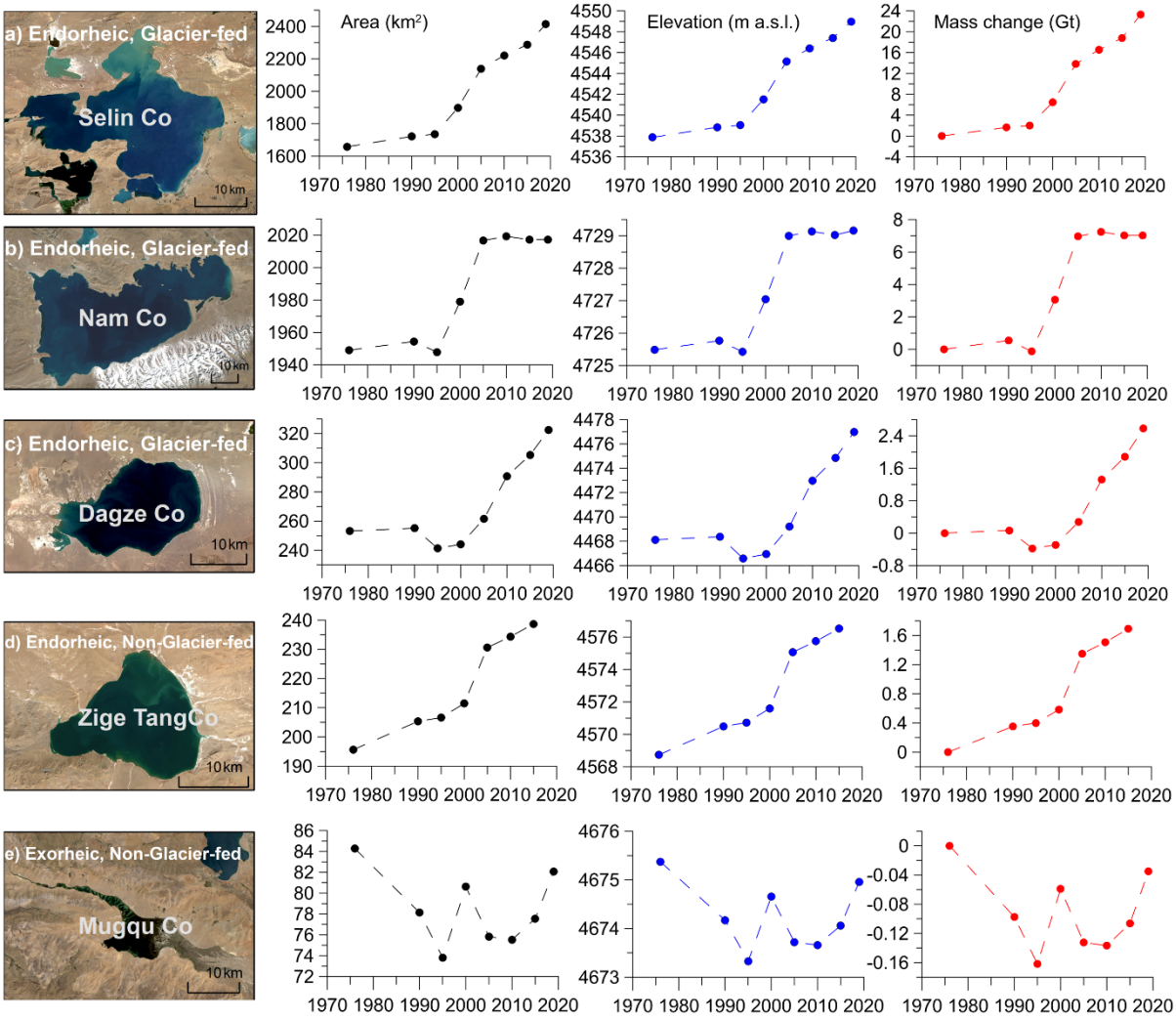

316 **Fig. 7**. Examples show the lake shoreline, time series of lake area, elevation and changes in lake mass between 1976
317 and 2019. The locations of these lakes are labeled in Fig. 1. The absolute elevation of lake level is provided here to
318 show the coherent time series along with lake area and water mass change, although the more reliable lake level
319 change is used to estimate water mass change in this study. Changes of the shoreline for Selin Co as an example
320 between 1976 and 2019 are provided in Fig. S2.
321
322 In 2019, most lakes have expanded in area relative to 1976, excluding some lakes in the southern TP (Fig. 8).
323 When the lakes are aggregated by different sizes (inset of Fig. 8), all lakes show a total area enlargement of ~27%, but
324 with larger relative augmentations for small lakes. Lake level changes show a consistent pattern with lake area. The
325 lake basin-wide decline of water level (-7 to 0 m) in the southern TP (<32°N) is smaller than the magnitude of water
326 level rise (0 to ~20 m) in the northern TP (>32°N). An abnormal small positive lake level change in Yamzho Yumco
327 basin could be due to lake level rising of a small lake in this basin and basin-wide mean water level is used (Fig. 8b).
328 On average, all lakes underwent a lake level rise of ~2.5 m, with higher increases for larger lakes. Again, the spatial
329 pattern of lake volume change is apparent, i.e., the magnitude of lake-water gain (0 to 23 Gt) against water loss (-5 to
330 0 Gt). Large lakes (>100 km^2) have greater positive water balances (21 to 58 Gt) than small lakes (2 to ~18 Gt).
331 Overall, the spatial patterns of lake area, level and volume change show a predominant amount of increases in the
332 northern TP (>32 °N) and decreases in the southern TP (<32 °N).
333 Spatial characteristics of lake volume changes are heterogeneous (Fig. 9). Most basins (274 of 429, 64%) contain
334 endorheic lakes (Fig. 9a); 129 basins have glacier meltwater supply lakes (Fig. 9b); and 113 basins have lakes both
335 endorheic and glacier-fed (Fig. 9c). The contrasting pattern (increasing versus decreasing, magnitude) of lake volume
336 change is clearer, with larger basin having greater lake water gain or loss. Among endorheic lakes and glacier-fed
337 lakes, lakes of almost all sizes experienced aggregative water gains (inset of Fig. 9c).
338
339

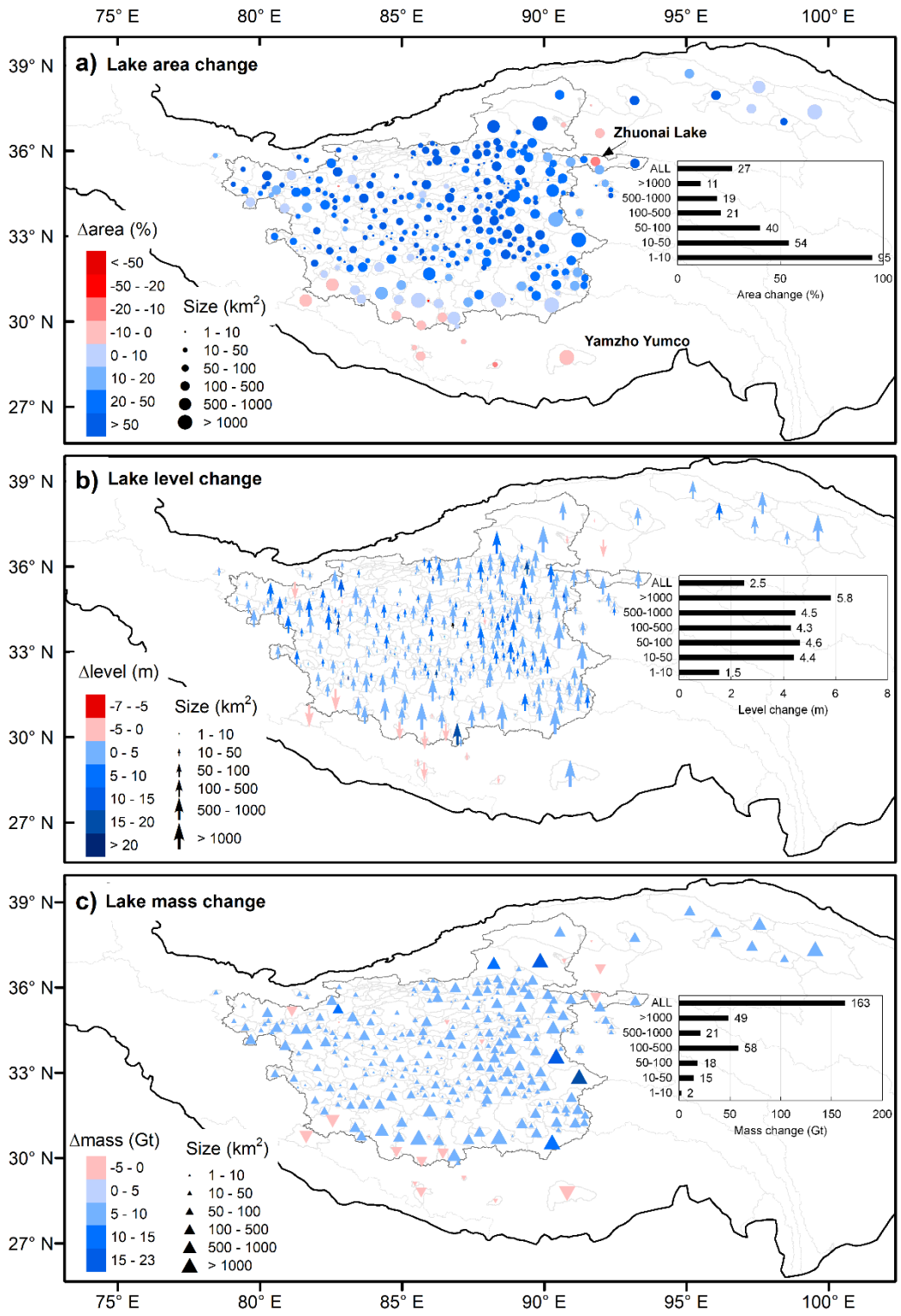

Fig. 8. Spatial pattern of lake area, level and mass changes between 1976 and 2019. Changes in lake area, level and mass are aggregated at each lake basin scale. The insets show the total area, mean level and total mass changes for different lake sizes.

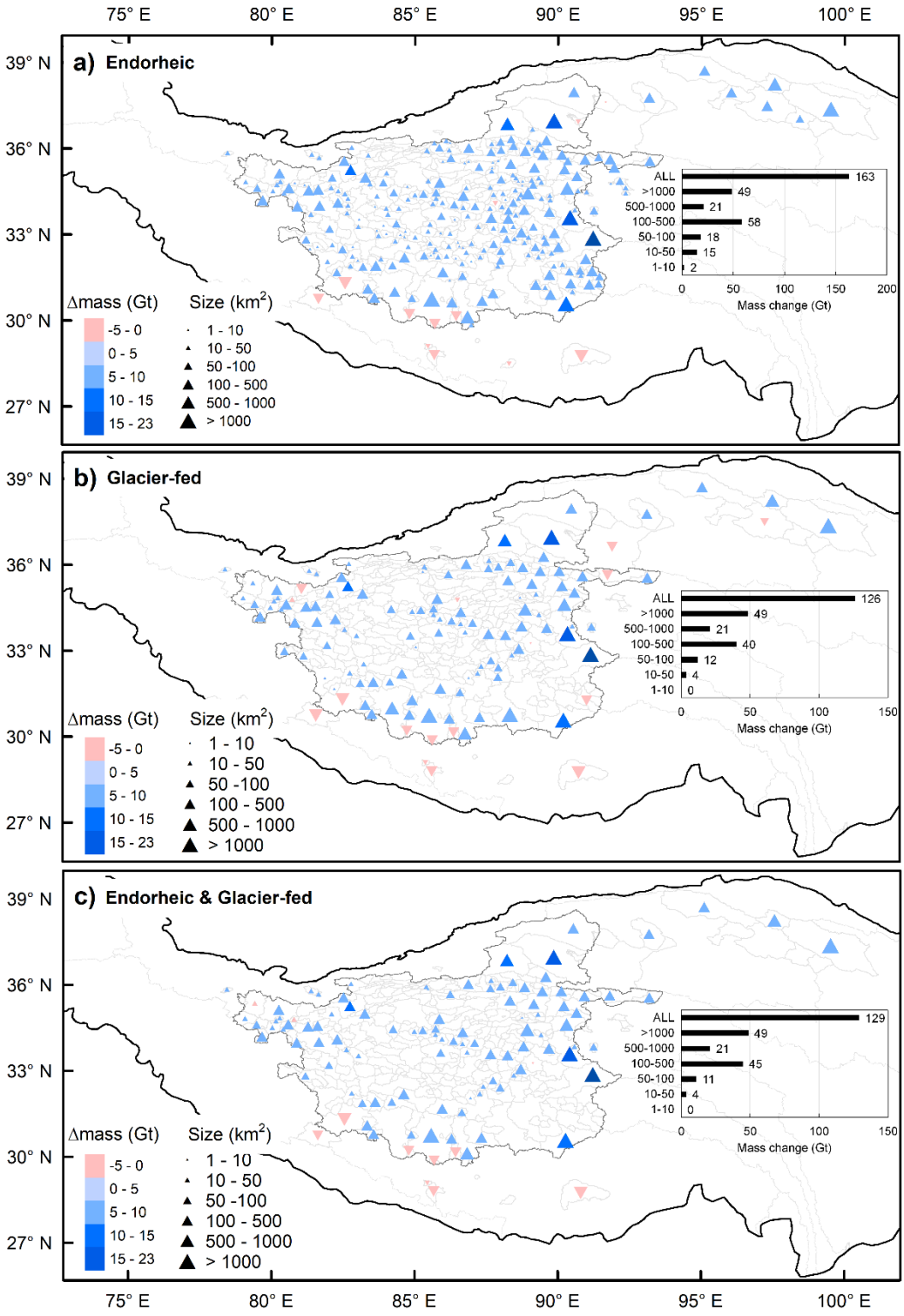

Fig. 9. Lake mass changes between 1976 and 2019 for endorheic lakes, glacier-fed lakes, and lakes that are both endorheic and glacier-fed for the different size classes. Lake mass change is aggregated for each lake basin. The insets show the total mass changes for endorheic lakes, glacier-fed lakes, and lakes that are both endorheic and glacier-fed.

4.3. Contribution of glacier mass loss to lake volume change

The spatial heterogeneity of the glacier mass balance within the lake basins follows the results summarized by Brun et al. (2017): Glaciers in lake basins of the northwestern TP have positive mass balances while those in the southern and northeastern TP show negative mass balances (Fig. 10a). For example, clear mass losses are observed for Nam Co and Selin Co basins (inset of Fig. 10a), with glacier mass balances of -0.41±0.16 and -0.39±0.17 m yr^{-1}, respectively.

The contribution of glacier mass loss to lake changes were quantitatively evaluated for 22 lake basins (Table 2 and Fig. 10b). The percentage of sampled area of glaciers within a lake basin ranges from 70.0% to 96.1%, with a mean of 86.4%. For fourteen basins the glacier contribution to lake volume increase is less than 30%, spanning from 0.3% to 29.1% with a mean of 11.6%. The remaining eight basins exhibited a greater glacier mass loss relative to lake water gain, with ratios from 116.3% to 435.6% (a mean of 203.0%). The lake volume increase from glacier contribution for two largest lakes in Tibet, Selin Co and Nam Co, are 28.4% and 8.2%, respectively.

For the Inner-TP as a whole, the lake mass change is 6.7±0.5 Gt yr^{-1} between 2000 and 2015 and 7.8±0.5 Gt yr^{-1} between 2000 and 2019. The excess glacier meltwater runoff in the Inner-TP is -1.5±0.5 Gt yr^{-1} during 2000−2016 (Brun et al., 2017), and -1.12±0.29 Gt yr^{-1} during 2000−2018 (Shean et al., 2020). Therefore, the relative contribution of glacier mass loss to lake mass increase is ~22% in 2000−2015 and ~14% in 2000−2019. In addition, a recent study reported that the glacier mass loss of -2.22±0.53 Gt yr^{-1} in 2010−2019 from CryoSat-2 observation (Jakob et al., 2020). The ratio of glacier contribution to lake water gain (7.2±0.8 Gt yr^{-1}) would be ~30% during 2010−2019. The ratio differences of glacier contribution could be reason of the glaciers coverage with available altimetry data, different study period, and boundary of Inner Tibet used. The remaining factors (precipitation–evaporation, snow and permafrost) would contribute a major fraction (>70%) of lake water gain.

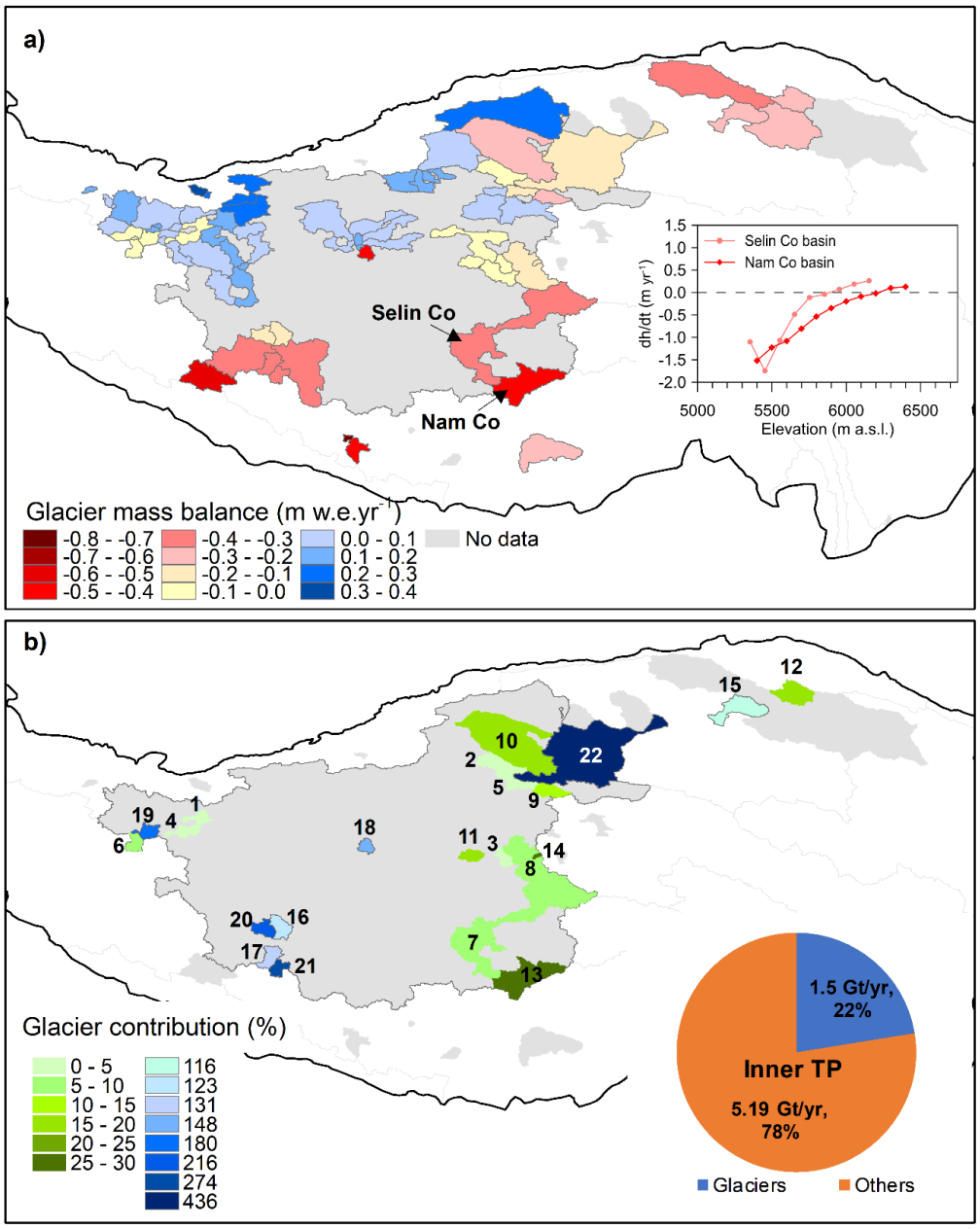

371

372 **Fig. 10**. Contribution of glacier mass balance to lake mass change between 2000 and ~2015. a) Glacier mass balance
373 at lake basin scale. The inset shows the altitude distribution of glacier elevation changes in lake basins of Selin Co and
374 Nam Co. b) Relative contribution (%) of glacier mass loss to lake mass increase. The inset shows that overall ratio of
375 glacier mass loss to lake mass change in the Inner-TP. The number (1 to 22) corresponds with values in Table 2.

376

377

378

Table 2 Contribution of glacier mass loss to lake mass changes between 2000 and ~2015 for endorheic lake basins.

No.	Lake name	Glacier area (km^2)	Basin area (km^2)	Sampled glacier area (%)	Lake mass change (Gt yr^{-1})	Glacier mass balance (m w.e. yr^{-1})	Glacier mass balance (Gt yr^{-1})	% of glacier to lake mass change
1	Bangdag Co	107.1	3613	91.0	0.08±0.05	-0.002±0.15	-0.0002±0.02	0.3
2	Jingyu Lake	62.7	4844	81.3	0.14±0.05	-0.01±0.16	-0.001±0.01	0.7
3	Meriqancomari	17.0	1555	90.4	0.03±0.04	-0.05±0.18	-0.001±0.003	3.1
4	Longjiao Co	4.2	343	94.7	0.003±0.013	-0.02±0.24	-0.0001±0.001	3.7
5	Lexie Wudan Lake	63.3	2019	77.7	0.15±0.05	-0.10±0.16	-0.01±0.01	4.4
6	Chem Co	186.8	1784	93.9	0.02±0.05	-0.01±0.14	-0.002±0.03	7.0
7	Selin Co	170.7	29057	80.0	0.82±0.19	-0.39±0.15	-0.07±0.03	8.2
8	Chibzhang Co	245.4	9888	85.0	0.57±0.11	-0.19±0.15	-0.05±0.04	8.3
9	Hoh Xil Lake	74.8	2637	79.8	0.11±0.09	-0.22±0.16	-0.02±0.01	14.8
10	Ayakkum Lake	339.8	24156	70.0	0.46±0.11	-0.23±0.16	-0.08±0.05	16.9
11	Lingo Co	142.7	1834	75.4	0.05±0.05	-0.07±0.15	-0.01±0.02	18.0
12	Hala Lake	79.4	4741	89.8	0.10±0.09	-0.24±0.15	-0.02±0.01	18.8
13	Nam Co	182.0	10730	84.6	0.26±0.19	-0.41±0.16	-0.08±0.03	28.4
14	Ug Co	9.3	277	81.4	0.004±0.022	-0.13±0.24	-0.001±0.002	29.1
15	Xiaochaidamu Lake	80.9	5814	86.9	0.02±0.01	-0.26±0.16	-0.02±0.01	116.3
16	Cam Co	100.0	2725	94.5	0.01±0.03	-0.17±0.14	-0.017±0.015	122.5
17	Rinqin Xubco	120.6	257	95.2	0.03±0.06	-0.32±0.15	-0.04±0.02	130.9
18	Garkung Caka	15.9	1280	88.6	0.005±0.002	-0.42±0.20	-0.007±0.003	147.8
19	Songmuxi Co	145.8	1904	94.4	0.002±0.002	-0.03±0.15	-0.004±0.02	180.2
20	Gopug Co	38.1	2329.5	95.0	0.003±0.003	-0.15±0.16	-0.006±0.006	216.1
21	Palung Co	71.6	1734	96.1	0.01±0.05	-0.33±0.15	-0.02±0.01	274.3
22	Taiyang Lake	716.2	34106	75.4	0.02±0.04	-0.10±0.14	-0.07±0.10	435.6

5. Discussion

5.1. Lake water balance from cryosphere and climate contributions

During 1976−2019, the TP lakes larger than 1 km^2 have increased in mass by a total of 169.7±15.1 Gt (3.9±0.4 Gt yr^{-1}). After 1995 a more noticeable increase of 214.9±12.7 Gt (9.0±0.5 Gt yr^{-1}) occurred, following a period of decrease (-45.2±8.2 Gt or -2.4±0.4 Gt yr^{-1}) between 1976 and 1995. This increase in water supply may have been the result of a changed climate (Kuang et al., 2016; Yang et al., 2014), either directly or indirectly through a changed cryospheric contribution (Bolch et al., 2019; Brun et al., 2017; Neckel et al., 2014; Shean et al., 2020; Yang et al.,

2019). Here, we quantified the glacier contribution at lake-basin scale using high-resolution (30 m) map of glacier elevation changes derived from ASTER DEMs (Brun et al., 2017). The magnitude of glacier mass balance for Nam Co basin (-0.41±0.16 m yr^{-1}) from ASTER stereo-imagery agree well with rate of -0.46±0.07 m yr^{-1} from an independent estimate based on TerraSAR-X/TanDEM-X observations (Zhang et al., 2017c). The glacier contribution for Selin Co is ~8.2%, which is similar to the result of ~10% between 2003 and 2012 from a distributed hydrological model (Zhou et al., 2015). Combining with basin-wide estimate for the entire Inner TP, our study draws a robust conclusion that glacier mass loss contributes a smaller fraction compared to other factors (>70%).

The lake water mass change in 2000–2010 in the Inner-TP (an endorheic basin) was 8.3±0.5 Gt yr^{-1}. The predominant amount of the terrestrial water storage (TWS) anomaly from the Gravity Recovery and Climate Experiment (GRACE) measurement can be imputed to lake storage increase from more comprehensive estimate of this study instead of glaciers mass gain (Jacob et al., 2012). A recent study from Ciracì et al. (2020) demonstrated a positive glacier mass balance (2.0 ± 4 Gt/yr) for Inner-TP (East Kunlun, Inner Tibet, and Qilian Shan) from the GRACE and GRACE Fellow-On missions between 2002 and 2019. Again, this error message could due to lake mass gain as revealed by this study. The water balance of the Inner-TP can be simplified as the difference between precipitation and actual evaporation, as the runoff depth is zero. According to earlier studies, the net precipitation (precipitation minus evaporation) is the dominant fraction (~70%) of TWS changes from GRACE observation in 2002–2015 (Yao et al., 2018; Zhang et al., 2017b). Lake volume changes examined in this study with more lakes and extended period relative to previous studies (Qiao et al., 2019b; Yang et al., 2017; Yao et al., 2018) and lake-basin scale estimates of glacier contribution further quantitatively confirms this conclusion.

The spatial pattern and time series of precipitation variations in our study area are shown in Fig. 11. From 1972 to 2015, the eastern TP became wetter and the southern margin of TP became drier. The precipitation variation is divided into two periods to match the apparent turning point in lake evolution. During 1972–1994, the overall precipitation change is negative. However, during 1995–2015, with the exception of southern periphery, it transformed into a positive trend. The time series trend of precipitation change is also apparent, with overall an increase of 0.93±0.34 mm yr^{-1} (P<0.01) in 1972–2015, a decrease of -0.83±0.87 mm yr^{-1} (P>0.1) in 1972–1994, but an increase of 0.81±0.98 mm yr^{-1} (P>0.1) in 1995–2015. The temporal and spatial patterns of precipitation variation (Fig. 11) generally match well with lake area, level and volume changes (Figs. 8 and 9).

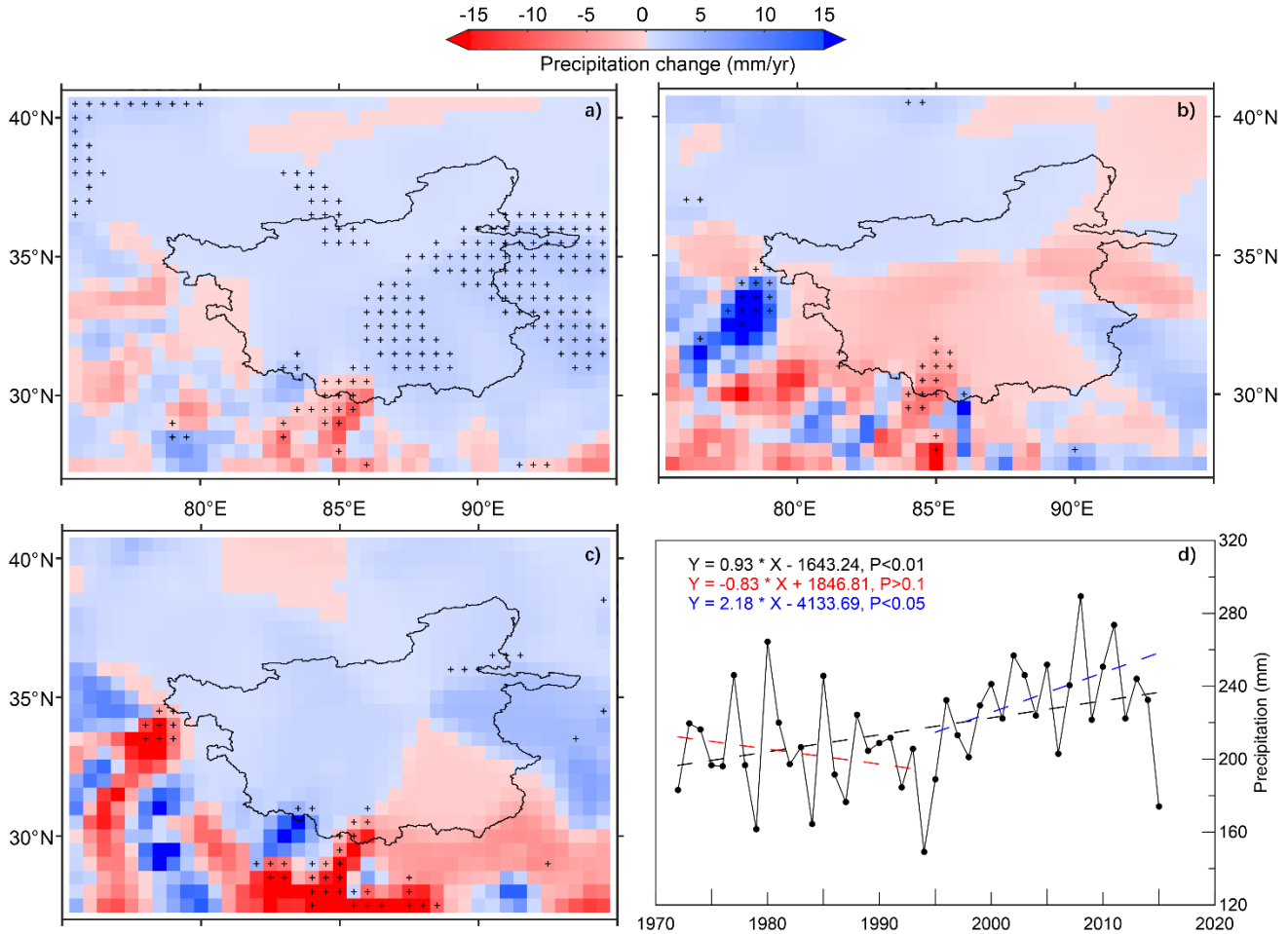

Fig. 11. Precipitation changes (mm yr^{-1}) around the Inner-TP from GPCC data. a) Spatial pattern of precipitation changes between 1972 and 2015. b) Spatial pattern of precipitation changes between 1972 and 1994. c) Spatial pattern of precipitation changes between 1995 and 2015. d) The time series of precipitation change (1972–1994 in red, 1995–2015 in blue) in the Inner-TP. The "+" indicates trends that are significant at the 95% level.

The time series of lake volume change is compared with cumulative standardized precipitation in Fig. 12. The lake volume change is related well with cumulative precipitation (r^2=0.95), which suggests that the increase in lake water can be predominantly explained by the climate factor of enhanced precipitation. Moreover, the previous studies have indicated that snow melting and permafrost degradation can contribute only small fractions (Che et al., 2014; Dai et al., 2012; Oelke et al., 2007; Zhang et al., 2017b). The overall estimates of lake volume change and extensive lake-basin glacier contributions reveal that the increased precipitation has mainly driven the lake water gains.

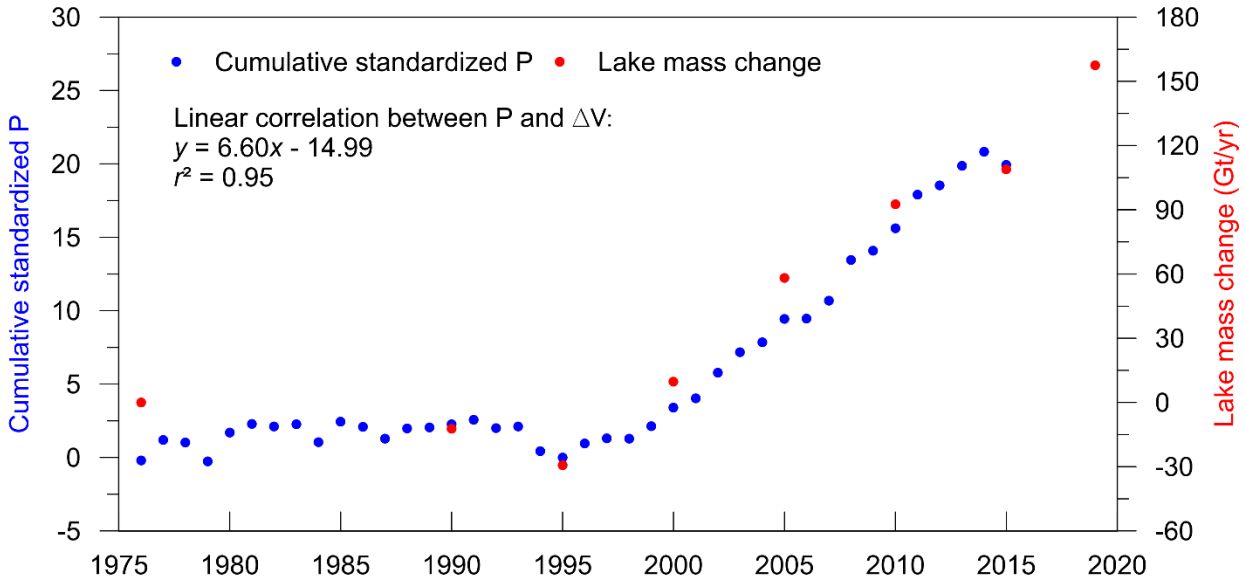

Fig. 12. The time series of cumulative standardized precipitation (P) from GPCC data and lake mass change (ΔV) in the Inner-TP. The equation of the linear fit between precipitation and ΔV is also shown.

5.2. Implication for the atmosphere and hydrological cycle

Several studies have already examined lake volume change and water balance of the TP (Crétaux et al., 2016; Qiao et al., 2019b; Song et al., 2013; Yang et al., 2017; Zhang et al., 2017b). However, this study provides the first comprehensively estimated individual lake (>1 km^2) volume change during 1976–2019. Lake area evolution agrees well with CMA-station observed precipitation change (Zhang et al., 2019). The time series of water level changes for several lakes with in situ lake level measurements are consistent with precipitation variations (Lei et al., 2014). The non-glacier-fed lakes showed fast water volume increase (Figs. 6 and 7), although the magnitude is smaller than for glacier-fed lakes. Recent quantitative studies of the water balance for several lakes (Mapam Yumco, Paiku Co, Tangra Yumco, Nam Co, Selin Co) (Biskop et al., 2016; Zhou et al., 2015) indicate that the glacier contribution to lake water gain is also less than 30% and this is confirmed by our results. The potential evapotranspiration in the TP has significantly declined due to reduced wind speed and a decrease in net total radiation, but actual evaporation has increased due to the warming (Yang et al., 2014; Zhang et al., 2007). Although the actual evaporation is increasing, the ratio of evaporation to precipitation indicates a decrease trending from 1982 to 2012 (Wang et al., 2018). The contribution of evaporation increase/decrease is greatly smaller relative to precipitation increase (Gao et al., 2015;

Guo et al., 2019; Lazhu et al., 2016; Ma et al., 2016). The lake volume change is therefore mainly driven by increased precipitation on the lake surface and the surrounding slopes within basin.

The lake volume changes derived here provide indirect evidence of the significant increase in the amount of precipitation. In addition, the increases in soil moisture content and vegetation activity also support the precipitation trend (Zhang et al., 2017d). Different precipitation products give different estimates of the trend in precipitation, but they present a general wetting trend (Kuang et al., 2016; Yang et al., 2018; Zhang et al., 2017a). The westerlies and the India summer monsoon transport most of the moisture over the TP. The increasing precipitation in the Inner-TP can be explained by enhanced water vapor convergence and redistribution by the local circulation (Curio et al., 2015; Gao et al., 2014; 2015; Yang et al., 2014; Zhang et al., 2017d). A recent study reveals that the positive phase of the Atlantic Multidecadal Oscillation (AMO) since the mid-1990s has led to increased precipitation in the Inner-TP since then (Sun et al., 2020). The summer precipitation in the southern TP is predominantly controlled by moisture evaporated elsewhere. The reduced precipitation in the southern TP is likely linked with a strong North Atlantic Oscillation, which weaken the moisture transport at the western boundary (Wang et al., 2017).

Significantly increased precipitation recycling over the TP implies an intensified hydrological cycle. The simulated runoff and surface soil moisture in the Inner-TP show increasing trends, except in the southern periphery where they are decreasing (Yang et al., 2011). The groundwater storage in the TP's endorheic basin derived from GRACE gravity data also provides evidence of an increasing TWS anomaly (Yi et al., 2016; Zhang et al., 2017b). This enhancement of the hydrological cycle is the response of the water resources (glaciers, snow cover, lakes and rivers) of the TP to warming and wetting (Chen et al., 2015). In the near future (2015–2050), the warming is projected to continue and more precipitation is expected (Zhu et al., 2013). It can therefore be expected that the lakes would continue to expand (Yang et al., 2018). This new hydrological regime could induce a series of hazards such as glacier collapse, flooding of pastures and roads, impacting on the local ecological environment and the livelihoods of local inhabitants.

6. Conclusions

Lakes on the TP are important indicators of environment change because they integrate the basin-wide variations of climate, cryosphere and ecosystems. This study provides a comprehensive estimate of lake volume changes in the TP between 1976 and 2019 using a robust algorithm to develop Elevation-Area correlation based on the DEMs and Landsat imageries. Lake-water storage in the past four decades has increased by 169.7±15.1 Gt. This increase

predominantly comes from the expansion of endorheic lakes (161.9±14.0 Gt). Both glacier-fed and non-glacier-fed lakes present water gains, but the magnitude of the increase in glacier-fed (127.1±14.3 Gt) is greater than that in non-glacier-fed lakes (42.6±4.9 Gt). This could be due to the increased precipitation as the dominant water input for both glacier-fed and non-glacier-fed lakes, and glacier mass loss as the additional supply for glacier-fed lakes. Lake-water mass gains have mainly occurred in the Inner-TP with an increase of 7.8±0.4 Gt yr^{-1} between 1995 and 2019. The spatial pattern of lake-basin scale is apparent, with increases for northern lakes (>32°N) predominantly located in the endorheic inner basin, but decreases for southern lakes (<32°N) predominantly located in the exorheic Brahmaputra basin. The contrasting pattern of lake volume change is clearer after lake classification by water supply mode such as endorheic lakes and glacier-fed lakes.

The glacier contribution to lake water balance was evaluated with state-of-the-art glacier mass balance at lake-basin scale. The northwestern lake basins have a positive glacier mass balance, but large negative glacier mass balances are found in the southern and eastern basins. The contributions of glacier loss to lake storage increase is less than 30% between 2000 and ~2019 for the Inner-TP as a whole, but variations are found between individual basins. The accumulated precipitation matched well with lake volume variations. This study reveals that the enhanced precipitation mainly drives lake volume increase but it is spatially heterogeneous.

The TP lakes would expand continuously in the near future as continued warming and wetting are expected. The quantitative assessment of lake-basin water balance from the other factors depends on available high-resolution climate and cryospheric observations by a hydrological model. This study opens the way to the routine estimation of future lake volume change and water balance in the TP, by synchronizing the climate and cryosphere datasets from in situ measurements, reanalysis and satellite data.

Acknowledgements

This study was supported by grants from the Natural Science Foundation of China (41831177, 41871056), the European Space Agency within the Dragon 4 program (4000121469/17/I-NB), the Swiss National Science Foundation (No. 200021E_177652/1), and the French Space Agency (CNES). G. Zhang wants to thank the China Scholarship Council for supporting his visit to University of Zurich (the former affiliation of T. Bolch) from December 2017 to December 2018. The authors also thank Fanny Brun, Etienne Berthier, and Kun Yang for their suggestions and helps

during the preparation of this manuscript. The 30-m SRTM DEM data used in this study are downloaded from NASA's Earth Science Data Systems (ESDS, https://earthdata.nasa.gov/). The Landsat imageries are from USGS EROS Data Center and NASA (https://glovis.usgs.gov). GPCC precipitation data is obtained from https://climatedataguide.ucar.edu/climate-data/gpcc-global-precipitation-climatology-centre. Landsat images used are provided in Table S1. Detailed information for 1132 lakes examined are provided in Table S2. Lake volume changes among different periods are provided in Table S3. We would like to thank three anonymous reviewers for the constructive comments to improve the paper.

Appendix A. Supplementary data

Supplementary data to this article can be found online.

References

Behrangi, A., Gardner, A.S., Reager, J.T., Fisher, J.B., 2017. Using GRACE to constrain precipitation amount over cold mountainous basins. Geophysical Research Letters. 44, 219-227.

Bhang, K.J., Schwartz, F.W., Braun, A., 2007. Verification of the vertical error in C-band SRTM DEM using ICESat and Landsat-7, Otter Tail County, MN. IEEE Transactions on Geoscience and Remote Sensing. 45, 36-44.

Biskop, S., Maussion, F., Krause, P., Fink, M., 2016. Differences in the water-balance components of four lakes in the southern-central Tibetan Plateau. Hydrol. Earth Syst. Sci. 20, 209−225.

Bolch, T., Peters, J., Yegorov, A., Pradhan, B., Buchroithner, M., Blagoveshchensky, V., 2011. Identification of potentially dangerous glacial lakes in the northern Tien Shan. Natural Hazards. 59, 1691-1714.

Bolch, T., Pieczonka, T., Mukherjee, K., Shea, J., 2017. Brief communication: Glaciers in the Hunza catchment (Karakoram) have been nearly in balance since the 1970s. The Cryosphere. 11, 531-539.

Bolch, T., Shea, J.M., Liu, S., Azam, F.M., Gao, Y., Gruber, S., et al. Status and Change of the Cryosphere in the Extended Hindu Kush Himalaya Region. In: Wester, P., Mishra, A., Mukherji, A., Shrestha, A.B., editors. The Hindu Kush Himalaya Assessment: Mountains, Climate Change, Sustainability and People. Springer International Publishing, Cham, 2019, pp. 209-255.

Brun, F., Berthier, E., Wagnon, P., Kääb, A., Treichler, D., 2017. A spatially resolved estimate of High Mountain Asia glacier mass balances from 2000 to 2016. Nature Geoscience. 10, 668-673.

Che, T., Li, X., Jin, R., Huang, C., 2014. Assimilating passive microwave remote sensing data into a land surface model to improve the estimation of snow depth. Remote Sensing of Environment. 143, 54-63.

Chen, D., Xu, B., Yao, T., Guo, Z., Cui, P., Chen, F., et al., 2015. Assessment of past, present and future environmental changes on the Tibetan Plateau. Chinese Science Bulletin. 60, 3025−3035.

Ciracì, E., Velicogna, I., Swenson, S., 2020. Continuity of the Mass Loss of the World's Glaciers and Ice Caps From the GRACE and GRACE Follow-On Missions. Geophysical Research Letters. 47.

Crétaux, J.F., Jelinski, W., Calmant, S., Kouraev, A., Vuglinski, V., Bergé-Nguyen, M., et al., 2011. SOLS: A lake database to monitor in the Near Real Time water level and storage variations from remote sensing data. Advances in Space Research. 47, 1497-1507.

Crétaux, J.F., Abarca-del-Río, R., Bergé-Nguyen, M., Arsen, A., Drolon, V., Clos, G., et al., 2016. Lake Volume Monitoring from Space. Surveys in Geophysics. 37, 269−305.

Curio, J., Maussion, F., Scherer, D., 2015. A 12-year high-resolution climatology of atmospheric water transport over the Tibetan Plateau. Earth System Dynamics. 6, 109-124.

Dai, L., Che, T., Wang, J., Zhang, P., 2012. Snow depth and snow water equivalent estimation from AMSR-E data based on a priori snow characteristics in Xinjiang, China. Remote Sensing of Environment. 127, 14-29.

Dai, Y., Wang, L., Yao, T., Li, X., Zhu, L., Zhang, X., 2018. Observed and Simulated Lake Effect Precipitation Over the Tibetan Plateau: An Initial Study at Nam Co Lake. Journal of Geophysical Research: Atmospheres. 123, 6746-6759.

Duan, A., Xiao, Z., 2015. Does the climate warming hiatus exist over the Tibetan Plateau? Scientific Reports. 5, 13711.

Farr, T.G., Rosen, P.A., Caro, E., Crippen, R., Duren, R., Hensley, S., et al., 2007. The Shuttle Radar Topography Mission. Rev. Geophys. 45, RG2004.

Fujita, K., Sakai, A., Nuimura, T., Yamaguchi, S., Sharma, R.R., 2009. Recent changes in Imja Glacial Lake and its damming moraine in the Nepal Himalaya revealed by in situ surveys and multi-temporal ASTER imagery. Environmental Research Letters. 4, 045205.

Gao, Y., Cuo, L., Zhang, Y., 2014. Changes in Moisture Flux over the Tibetan Plateau during 1979–2011 and Possible Mechanisms. Journal of Climate. 27, 1876-1893.

Gao, Y., Leung, L.R., Zhang, Y., Cuo, L., 2015. Changes in Moisture Flux over the Tibetan Plateau during 1979–2011: Insights from a High-Resolution Simulation. Journal of Climate. 28, 4185−4197.

Gardelle, J., Berthier, E., Arnaud, Y., 2012. Slight mass gain of Karakoram glaciers in the early twenty-first century. Nature Geosci. 322-325.

Gardner, A.S., Moholdt, G., Cogley, J.G., Wouters, B., Arendt, A.A., Wahr, J., et al., 2013. A Reconciled Estimate of Glacier Contributions to Sea Level Rise: 2003 to 2009. Science. 340, 852−857.

Guo, Y., Zhang, Y., Ma, N., Xu, J., Zhang, T., 2019. Long-term changes in evaporation over Siling Co Lake on the Tibetan Plateau and its impact on recent rapid lake expansion. Atmospheric Research. 216, 141-150.

Immerzeel, W.W., Lutz, A.F., Andrade, M., Bahl, A., Biemans, H., Bolch, T., et al., 2020. Importance and vulnerability of the world's water towers. Nature. 577, 364–369.

Jacob, T., Wahr, J., Pfeffer, W.T., Swenson, S., 2012. Recent contributions of glaciers and ice caps to sea level rise. Nature. 482, 514-518.

Jakob, L., Gourmelen, N., Ewart, M., Plummer, S., 2020. Ice loss in High Mountain Asia and the Gulf of Alaska observed by CryoSat-2 swath altimetry between 2010 and 2019. The Cryosphere Discuss. 2020, 1-29.

Jiang, L., Nielsen, K., Andersen, O.B., Bauer-Gottwein, P., 2017. Monitoring recent lake level variations on the Tibetan Plateau using CryoSat-2 SARIn mode data. Journal of Hydrology. 544, 109-124.

Kääb, A., Berthier, E., Nuth, C., Gardelle, J., Arnaud, Y., 2012. Contrasting patterns of early twenty-first-century glacier mass change in the Himalayas. Nature. 488, 495-498.

Kleinherenbrink, M., Lindenbergh, R.C., Ditmar, P.G., 2015. Monitoring of lake level changes on the Tibetan Plateau and Tian Shan by retracking Cryosat SARIn waveforms. Journal of Hydrology. 521, 119-131.

Kuang, X., Jiao, J.J., 2016. Review on climate change on the Tibetan Plateau during the last half century. Journal of Geophysical Research: Atmospheres. 121, 3979-4007.

Lazhu, Yang, K., Wang, J., Lei, Y., Chen, Y., Zhu, L., et al., 2016. Quantifying evaporation and its decadal change for Lake Nam Co, Central Tibetan Plateau. Journal of Geophysical Research: Atmospheres. 7578-7591.

Lei, Y., Yang, K., Wang, B., Sheng, Y., Bird, B.W., Zhang, G., et al., 2014. Response of inland lake dynamics over the Tibetan Plateau to climate change. Climatic Change. 125, 281−290.

Li, B., Zhang, J., Yu, Z., Liang, Z., Chen, L., Acharya, K., 2017a. Climate change driven water budget dynamics of a Tibetan inland lake. Global and Planetary Change. 150, 70-80.

Li, G., Lin, H., 2017b. Recent decadal glacier mass balances over the Western Nyainqentanglha Mountains and the increase in their melting contribution to Nam Co Lake measured by differential Bistatic SAR interferometry. Global and Planetary Change. 149, 177-190.

Li, J., Sheng, Y., 2012. An automated scheme for glacial lake dynamics mapping using Landsat imagery and digital elevation models: a case study in the Himalayas. International Journal of Remote Sensing. 33, 5194−5213.

Li, Q., Zhang, H., Liu, X., Chen, J., Li, W., Jones, P., 2009. A Mainland China Homogenized Historical Temperature Dataset of 1951–2004. Bulletin of the American Meteorological Society. 90, 1062-1065.

Ma, N., Szilagyi, J., Niu, G.-Y., Zhang, Y., Zhang, T., Wang, B., et al., 2016. Evaporation variability of Nam Co Lake in the Tibetan Plateau and its role in recent rapid lake expansion. Journal of Hydrology. 537, 27-35.

Marzeion, B., Cogley, J.G., Richter, K., Parkes, D., 2014. Attribution of global glacier mass loss to anthropogenic and natural causes. Science. 345, 919-921.

McFeeters, S.K., 1996. The use of the normalized difference water index (NDWI) in the delineation of open water features. International Journal of Remote Sensing. 17, 1425−1432.

Neckel, N., Kropáček, J., Bolch, T., Hochschild, V., 2014. Glacier mass changes on the Tibetan Plateau 2003–2009 derived from ICESat laser altimetry measurements. Environmental Research Letters. 9, 014009.

Niu, Z., Zhang, H., Gong, P., 2011. More protection for China's wetlands. Nature. 471, 305-305.

Oelke, C., Zhang, T., 2007. Modeling the Active-Layer Depth over the Tibetan Plateau. Arctic, Antarctic, and Alpine Research. 39, 714-722.

Otsu, N., 1979. A Threshold Selection Method from Gray-Level Histograms. IEEE Transactions on Systems, Man and Cybernetics. 9, 62−66.

Pekel, J.-F., Cottam, A., Gorelick, N., Belward, A.S., 2016. High-resolution mapping of global surface water and its long-term changes. Nature. 540, 418−422.

Pfeffer, W.T., Arendt, A.A., Bliss, A., Bolch, T., Cogley, J.G., Gardner, A.S., et al., 2014. The Randolph Glacier Inventory: a globally complete inventory of glaciers. Journal of Glaciology. 60, 537-552.

Phan, V.H., Lindenbergh, R., Menenti, M., 2012. ICESat derived elevation changes of Tibetan lakes between 2003 and 2009. International Journal of Applied Earth Observation and Geoinformation. 17, 12−22.

Qiao, B., Zhu, L., Wang, J., Ju, J., Ma, Q., Huang, L., et al., 2019a. Estimation of lake water storage and changes based on bathymetric data and altimetry data and the association with climate change in the central Tibetan Plateau. Journal of Hydrology. 578, 124052.

Qiao, B., Zhu, L., Yang, R., 2019b. Temporal-spatial differences in lake water storage changes and their links to climate change throughout the Tibetan Plateau. Remote Sensing of Environment. 222, 232-243.

Rabus, B., Eineder, M., Roth, A., Bamler, R., 2003. The shuttle radar topography mission--a new class of digital elevation models acquired by spaceborne radar. ISPRS Journal of Photogrammetry and Remote Sensing. 57, 241-262.

RGI-Consortium. Randolph Glacier Inventory, A Dataset of Global Glacier Outlines: Version 6.0. Technical Report, 2017.

Rodriguez, E., Morris, C.S., Belz, J.E., 2006. A global assessment of the SRTM performance. Photogrammetry Engineering and Remote Sensing. 72, 249-260.

Rüthrich, F., Reudenbach, C., Thies, B., Bendix, J., 2015. Lake-Related Cloud Dynamics on the Tibetan Plateau: Spatial Patterns and Interannual Variability. Journal of Climate. 28, 9080-9104.

Salerno, F., Thakuri, S., D'Agata, C., Smiraglia, C., Manfredi, E.C., Viviano, G., et al., 2012. Glacial lake distribution in the Mount Everest region: Uncertainty of measurement and conditions of formation. Global and Planetary Change. 92–93, 30-39.

Samuelsson, P., Kourzeneva, E., Mironov, D., 2010. The impact of lakes on the European climate as stimulated by a regional climate madel. Boreal environment research. 15, 113-119.

Scaramuzza, P., Scaramuzza, E., Scaramuzza, G. SLC gap-filled products: Phase one methodology, http://landsat.usgs.gov/documents/SLC_Gap_Fill_Methodology.pdf, 2004.

Shean, D.E., Bhushan, S., Montesano, P., Rounce, D.R., Arendt, A., Osmanoglu, B., 2020. A Systematic, Regional Assessment of High Mountain Asia Glacier Mass Balance. Frontiers in Earth Science. 7.

Sheng, Y., Song, C., Wang, J., Lyons, E.A., Knox, B.R., Cox, J.S., et al., 2016. Representative lake water extent mapping at continental scales using multi-temporal Landsat-8 imagery. Remote Sensing of Environment. 185, 129-141.

Song, C., Huang, B., Ke, L., 2013. Modeling and analysis of lake water storage changes on the Tibetan Plateau using multi-mission satellite data. Remote Sensing of Environment. 135, 25−35.

Sun, J., Yang, K., Guo, W., Wang, Y., He, J., Lu, H., 2020. Why has the Inner Tibetan Plateau become wetter since the mid-1990s? Journal of Climate. 33, 8507-8522.

Tian, P., Lu, H., Feng, W., Guan, Y., Xue, Y., 2020. Large decrease in streamflow and sediment load of Qinghai–Tibetan Plateau driven by future climate change: A case study in Lhasa River Basin. Catena. 187.

Tong, K., Su, F., Yang, D., Zhang, L., Hao, Z., 2014. Tibetan Plateau precipitation as depicted by gauge observations, reanalyses and satellite retrievals. International Journal of Climatology. 34, 265-285.

Tong, K., Su, F., Li, C., 2020. Modeling of Water Fluxes and Budget in Nam Co Basin during 1979–2013. Journal of Hydrometeorology. 21, 829-844.

Treichler, D., Kääb, A., Salzmann, N., Xu, C.-Y., 2019. Recent glacier and lake changes in High Mountain Asia and their relation to precipitation changes. The Cryosphere. 13, 2977-3005.

Verpoorter, C., Kutser, T., Seekell, D.A., Tranvik, L.J., 2014. A Global Inventory of Lakes Based on High-Resolution Satellite Imagery. Geophysical Research Letters. 41, 6396−6402.

Wang, W., Li, J., Yu, Z., Ding, Y., Xing, W., Lu, W., 2018. Satellite retrieval of actual evapotranspiration in the Tibetan Plateau: components partitioning, multidecadal trends and dominated factors identifying. Journal of Hydrology. 559, 471-485.

Wang, X., Ding, Y., Liu, S., Jiang, L., Wu, K., Jiang, Z., et al., 2013. Changes of glacial lakes and implications in Tian Shan, central Asia, based on remote sensing data from 1990 to 2010. Environmental Research Letters. 8, 044052.

Wang, Z., Duan, A., Yang, S., Ullah, K., 2017. Atmospheric moisture budget and its regulation on the variability of summer precipitation over the Tibetan Plateau. Journal of Geophysical Research: Atmospheres. 122, 614-630.

Williamson, C.E., Saros, J.E., Vincent, W.F., Smol, J.P., 2009. Lakes and reservoirs as sentinels, integrators, and regulators of climate change. Limnology and Oceanography. 54, 2273-2282.

Wortmann, M., Bolch, T., Menz, C., Tong, J., Krysanova, V., 2018. Comparison and Correction of High-Mountain Precipitation Data Based on Glacio-Hydrological Modeling in the Tarim River Headwaters (High Asia). Journal of Hydrometeorology. 19, 777-801.

Xiang, L., Wang, H., Steffen, H., Wu, P., Jia, L., Jiang, L., et al., 2016. Groundwater storage changes in the Tibetan Plateau and adjacent areas revealed from GRACE satellite gravity data. Earth and Planetary Science Letters. 449, 228-239.

Yamazaki, D., Trigg, M.A., Ikeshima, D., 2015. Development of a global ~ 90 m water body map using multi-temporal Landsat images. Remote Sensing of Environment. 171, 337−351.

Yang, K., Ye, B., Zhou, D., Wu, B., Foken, T., Qin, J., et al., 2011. Response of hydrological cycle to recent climate changes in the Tibetan Plateau. Climatic Change. 109, 517−534.

Yang, K., Wu, H., Qin, J., Lin, C., Tang, W., Chen, Y., 2014. Recent climate changes over the Tibetan Plateau and their impacts on energy and water cycle: A review. Global and Planetary Change. 112, 79−91.

Yang, K., Lu, H., Yue, S., Zhang, G., Lei, Y., Zhu, L., et al., 2018. Quantifying recent precipitation change and predicting lake expansion in the Inner Tibetan Plateau. Climatic Change. 147, 149-163.

Yang, M., Wang, X., Pang, G., Wan, G., Liu, Z., 2019. The Tibetan Plateau cryosphere: Observations and model simulations for current status and recent changes. Earth-Science Reviews. 190, 353-369.

Yang, R., Zhu, L., Wang, J., Ju, J., Ma, Q., Turner, F., et al., 2017. Spatiotemporal variations in volume of closed lakes on the Tibetan Plateau and their climatic responses from 1976 to 2013. Climatic Change. 140, 621-633.

Yao, F., Wang, J., Yang, K., Wang, C., Walter, B., Cretaux, J.-F., 2018. Lake storage variation on the endorheic Tibetan Plateau and its attribution to climate change since the new millennium. Environmental Research Letters. 13, 064011.

673 Yi, S., Wang, Q., Sun, W., 2016. Basin mass dynamic changes in China from GRACE based on a multi-basin inversion
674 method. Journal of Geophysical Research: Solid Earth. 121, 3782-3803.
675 Yu, J., Zhang, G., Yao, T., Xie, H., Zhang, H., Ke, C., et al., 2016. Developing daily cloud-free snow composite products
676 from MODIS Terra-Aqua and IMS for the Tibetan Plateau. IEEE Transactions on Geoscience and Remote Sensing.
677 54, 2171−2180.
678 Zhang, C., Tang, Q., Chen, D., 2017a. Recent changes in the moisture source of precipitation over the Tibetan Plateau.
679 Journal of Climate. 30, 1807-1819.
680 Zhang, G., Xie, H., Kang, S., Yi, D., Ackley, S., 2011. Monitoring lake level changes on the Tibetan Plateau using ICESat
681 altimetry data (2003−2009). Remote Sensing of Environment. 115, 1733−1742.
682 Zhang, G., Yao, T., Shum, C.K., Yi, S., Yang, K., Xie, H., et al., 2017b. Lake volume and groundwater storage variations in
683 Tibetan Plateau's endorheic basin. Geophysical Research Letters. 44, 5550-5560.
684 Zhang, G., Luo, W., Chen, W., Zheng, G., 2019. A robust but variable lake expansion on the Tibetan Plateau. Science
685 Bulletin. 64, 1306-1309.
686 Zhang, G., Yao, T., Xie, H., Yang, K., Zhu, L., Shum, C.K., et al., 2020. Response of Tibetan Plateau lakes to climate
687 change: Trends, patterns, and mechanisms. Earth-Science Reviews. 208, 103269.
688 Zhang, Q., Zhang, G., 2017c. Glacier elevation changes in the western Nyainqentanglha Range of the Tibetan Plateau as
689 observed by TerraSAR-X/TanDEM-X images. Remote Sensing Letters. 8, 1143-1152.
690 Zhang, W., Zhou, T., Zhang, L., 2017d. Wetting and greening Tibetan Plateau in early summer in recent decades. Journal of
691 Geophysical Research: Atmospheres. 122, 5808-5822.
692 Zhang, Y., Liu, C., Tang, Y., Yang, Y., 2007. Trends in pan evaporation and reference and actual evapotranspiration across
693 the Tibetan Plateau. J. Geophys. Res. 112, D12110.
694 Zhong, L., Ma, Y., Xue, Y., Piao, S., 2019. Climate Change Trends and Impacts on Vegetation Greening Over the Tibetan
695 Plateau. Journal of Geophysical Research: Atmospheres. 124, 7540-7552.
696 Zhou, J., Wang, L., Zhang, Y., Guo, Y., Li, X., Liu, W., 2015. Exploring the water storage changes in the largest lake (Selin
697 Co) over the Tibetan Plateau during 2003–2012 from a basin-wide hydrological modeling. Water Resources Research.
698 51, 8060−8086.
699 Zhou, Y., Hu, J., Li, Z., Li, J., Zhao, R., Ding, X., 2019. Quantifying glacier mass change and its contribution to lake
700 growths in Central Kunlun during 2000-2015 from multi-source remote sensing data. Journal of Hydrology. 570, 38-
701 50.

Zhu, L., Jin, J., Liu, X., Tian, L., Zhang, Q., 2018. Simulations of the Impact of Lakes on Local and Regional Climate Over the Tibetan Plateau. Atmosphere-Ocean. 56, 230-239.

Zhu, X., Wang, W., Fraedrich, K., 2013. Future Climate in the Tibetan Plateau from a Statistical Regional Climate Model. Journal of Climate. 26, 10125-10138.

Zhu, Z., Piao, S., Myneni, R.B., Huang, M., Zeng, Z., Canadell, J.G., et al., 2016. Greening of the Earth and its drivers. Nature Clim. Change. 6, 791-795.